NTNU – Trondheim
Norwegian University of
Science and Technology

Building, Testing and Qualifying New Hook Load Rig

Asgeir Sogge Sjøberg

Petroleum Geoscience and Engineering
Submission date: June 2014
Supervisor: Pål Skalle, IPT

Norwegian University of Science and Technology
Department of Petroleum Engineering and Applied Geophysics

Abstract

To meet the growing demand for energy, the petroleum industry is looking in places previously thought to be unreachable. The continued search is causing the oil and gas industry to drill more advanced wells than ever. With the increased challenges of drilling, non-productive time (NPT) is a rising concern for the industry. During drilling, NPT annually amounts to as much as 35% of the costs of the operation. Therefore, identifying and understanding variations in the drilling parameters during drilling operations is important. Recognizing well signals and signatures will enable early problem detection, thereby reduce NPT, and enhance safety.

This thesis concentrates on initial investigations into hook load variations during tripping out of hole and thereafter make a laboratory model for hook load simulation. This in order to contribute to the understanding of the signals given by variations in hook load values. A hook load rig is developed based on the theory presented and previous hook load models built at NTNU. The apparatus consisted of elements representing the drilling rig hoisting system, low-pressure mud circulation system, the drillstring including bottom hole assembly, the borehole and relevant controls and instrumentation.

Detailed procedures for use of the hook load rig are established and presented. A program to monitor and control the experiments was made in LabVIEW. The model encompasses large pulling force capacity and safety features to safeguard its operation, as well as flexibility with respect to key parameter variations. Several experiments have been performed in the laboratory order to qualify the rig. Tests with restrictions and without restrictions were conducted in order to identify hook load signatures. Issues, such as frequency disturbances were investigated and largely resolved.

The results presented in this thesis have identified curves resembling real-time drilling data for normal hook load, cuttings accumulation, and for moving past an obstacle by laboratory simulations. In its current state, the hook load rig provides for a solid foundation for further testing and experiments.

Sammendrag

For å møte verdens stadig økende energibehovet, leter olje- og gassindustrien etter ressurser på plasser som tidligere var utenkelige. Dette innebærer blant annet boring av brønner som er stadig mer avanserte. Med de økte utfordringene, er ikke-produktiv tid en økende bekymring. Ikke-produktiv tid står i gjennomsnitt for så mye som 35 % av boreoperasjonskostnadene. Derfor er det å identifisere og forstå betydningen av variasjoner i boreparametere viktig. Gjenkjenning av typiske brønnsignaler og signaturer bidrar til tidlig oppdagelse av mulige problemer slik at tiltak kan iverksettes. Dette vil redusere ikke-produktiv tid i tillegg til å øke sikkerheten ved operasjonen. Denne avhandlingen fokuserer på variasjoner i krok-last og deretter bygging av en laboratoriemodell for å simulere krok-last data. En krok-last rigg er bygget basert på teorien som blir fremlagt samt erfaringer fra en tidligere modell bygget ved NTNU. Laboratoriemodellen består av deler som representerer heise-spillet, lav-trykks sirkulasjonssystem, borestrengen og borehullet og relevante instrumenter og kontroll systemer.

Detaljerte prosedyrer for krok-last riggen er blitt laget og presentert. Et program for å overvåke og kontrollere eksperimentene er blitt laget i LabVIEW. Modellen har høy dra-kraft og funksjoner for å ivareta sikkerheten under bruk er derfor implementert. Eksperimenter er blitt utført i laboratoriet for å kvalifisere riggen. Tester med og uten borehullsrestriksjoner er utført for å etablere krok-last signaturer. Problemer som støy fra frekvensomformere ble identifisert, vurdert og i stor grad løst.

Resultatene i fra de utførte testene viser kurver for krok-last som overensstemmer med sann-tid boredata for normal krok-last, akkumulering av borekaks og bevegelse over en restriksjon. Den nye krok-last riggen danner således et solid fundament for videre oppgaver, tester og eksperimenter ved instituttet.

Preface

This thesis was written at the Department of Petroleum Engineering and Applied Geophysics at NTNU during the spring semester of 2014.

I would like to thank Jarle Glad for his invaluable assistance and contribution in building the laboratory model. As he is about to retire, I would like to extend my best wishes for him in the future. I would like to thank my professor, Pål Skalle, for his enthusiasm, good spirit and guidance during the course of this thesis. Further, a thank you goes out to Åge Sivertsen for his help with the electrical components. In addition, I would like to thank my father, Geir Sjøberg at Aker Solutions, for his insight and assistance in industry related questions, and Ståle Færøy at Transocean and Tor Inge Waag at Aker Solutions/Drilling Technologies for great conversations and for answering my questions related to interference and signal disturbance on offshore installations.

Asgeir Sjøberg

Trondheim, June 2013

Table of Contents

Abstract iii
Sammendrag v
Preface vii
List of Figures xi
List of Tables xii
1 Introduction 1
2 Hook Load 3
2.1 Hook Load Hoisting System 3
2.2 Modern Hoisting systems 5
3 Physical Parameters Effecting Hook Load Measurements 7
3.1 Drillstring weight and buoyancy 7
3.2 Friction 9
3.2.1 Torque and drag derivation 11
3.2.2 Straight hole section 11
3.2.3 Curved hole section 12
3.2.4 Coefficient of Friction (CoF) 14
3.3 Fluid drag 16
3.4 Elalstic behavior 16
4 Hook Load Signatures during Tripping From Literature and RTDD 19
4.1 Normal hook load during tripping 21
4.2 Abnormal Hook Load readings 23
4.2.1 Pack offs 24
4.2.2 Differential sticking 28
4.2.3 Key seat, ledges and or dog leg 30
5 Previous published literature on Hook Load Evaluation 35
5.1 Monitoring of drilling parameters-The relevance of establishing symptom recognition models. 35
5.2 Previous work on Hook Load at NTNU 36
6 Hook load Model Experiment 41

6.1 Planning and execution summary 42
6.2 Design and building of hook load rig 46
6.2.1 Equipment 49
6.2.2 Electronics 55
6.3 Running the Experiments 56
6.3.1 Lab View 56
6.3.2 Procedures 62
6.4 Test matrix 64
7 Results of the Hook load model experiments 67
7.1 Trial runs: Interference Issue 68
7.2 Tests at normal hook load 70
7.3 Tests for evaluation of the data acquisition system 72
7.4 Testing with restrictions 74
8 Evaluation and Discussion 79
8.1 Evaluation of Hook load rig 79
8.2 Evaluation of Results 81
8.3 Further work 85
9 Conclusion 87
10 Nomenclature 89
11 Bibliography 91

List of Figures

Figure 1: Detailed hook load set-up on rig **4**
Figure 2: A rig set -up showing how hook load is measured **4**
Figure 3: Modern Hydraulic Ram Rig. **5**
Figure 4: BHA with typical components **8**
Figure 5: Forces in a straight borehole section **9**
Figure 6: Axial and rotational movement in the borehole **10**
Figure 7: Discreet model of torque and drag **13**
Figure 8: Static friction and kinetic friction as a factor of applied force **15**
Figure 9: Stress vs strain curve **18**
Figure 10: Planned vs actual wellpath **20**
Figure 11: Drillfloor with traveling block hoisted and ready to disconnect a stand **21**
Figure 12: From study by Cordoso et, al. indicating a normal hook load reading for one stand **22**
Figure 13: Normal hook load curve during POOH from RTDD data **23**
Figure 14: Cuttings jamming during tripping **24**
Figure 15: Overpull event from RTDD **26**
Figure 16: Increasing SPP indicating downhole restriction of flow **27**
Figure 17: Increase in SPP and erratic hook load curve when hoisting drillstring **28**
Figure 18: Differential sticking **29**
Figure 19: Hook load curve indicating differential sticking **30**
Figure 20: Indication of ledge **32**
Figure 21: Longer time-view of the overpull event, showing hard stringers before and after. **34**
Figure 22: Mass-spring model and its response to being pulled **36**
Figure 23: Hook load signatures while encountering restrictions during POOH **38**
Figure 24: Cuttings accumulation in from RTDD data **39**
Figure 25: Gnatt-diagram 25.03.2014 ..... **44**
Figure 26: Gantt-diagram showing progress as of 08.06.2014 ..... **45**
Figure 27: Potential Buckling Direction during pulling of Drillstring **46**
Figure 28: Rotated view of the complete setup of hook load rig **47**
Figure 29: Water/mud circulation system at each end of the borehole **48**
Figure 30: Jack and tighten clamp attached to drillstring to free stuck BHA **49**
Figure 31: Assembled winch **50**
Figure 32: Load cells/tension meters **51**
Figure 33: BHAs milled in the workshop. From left to right: BHA 3, BHA 1, and BHA 2 ..... **52**
Figure 34: Fluid seal for end of pipe **53**
Figure 35: Principle of added pulling length to the position meter **54**
Figure 36: Electronic schematics for hook load rig **55**

Figure 37: Block diagram with coding for running HKL test **58**
Figure 38: Rotated view of the front panel for monitoring of hook load experiments **61**
Figure 39: Flowchart for running Hook Load experiment **63**
Figure 40: Legend for graphs **67**
Figure 41: Different levels of interference **69**
Figure 42: Hook Load variation during slow, steady POOH speed **71**
Figure 43: Hook load tests with two different data acquisition rates. **73**
Figur 44: BHA moving over a restriction **75**
Figure 45: A stuck pipe simulation from cutting accumulation **77**
Figure 46: Figures resembling the established fingerprints for hook loads **82**
Figure 47: Interference on the hook load signal. **83**

List of Tables

Table 1: Planned vs actual drilling operation times **19**
Table 2: Weight and dimensions of HKL equipment **52**
Table 3: Test matrix from initial trails **65**
Table 4: Final test matrix for experiments **66**

1 Introduction

Energy is today an essential part of human life. Energy has been and will continue to be at the core of all technology and human innovation. The continued growth of the human population, improved standards of living amongst people, particularly in India and the Far East and the related technology development mean the energy demand will continue to grow.

To meet this demand the petroleum industry is looking for energy in places previously thought to be unreachable. There is a need to constantly push the envelope of technical innovation and creative solutions. In a world where hydrocarbon resources are being depleted, the continued search is causing the oil and gas industry to drill more advanced wells than ever.

The industry has seen major improvements in recent years in every aspect of drilling. Reservoirs and wells that would have been impossible a few decades ago are now being drilled and completed successfully. Major achievements have been possible by the introduction of the top drive in the -80's, followed by improved technology for directional control and geology evaluation while drilling. However, new technical challenges are rising. Core to any drilling operation is the actual making of the wellbore in a safe and efficient manner. Most of the problems related to directional drilling occur during tripping (Cordoso Jr et al., 1995). During the monitoring of operational parameters, one of the most important is the hook load. A shift in hook look will signal a change in the borehole.

Due to the importance of monitoring the borehole during drilling operations, identifying changes can increase profits and safety.

At NTNU the goal is to bring the field into the laboratory, in order to simulate real world results. By mirroring the field conditions as closely as possible in the laboratory, we can investigate causes of problems and try to find solutions.

This thesis concentrates on initial investigations into hook load variations and thereafter make a laboratory model for hook load simulation in order to contribute to the understanding of the signals given by variations in hook load values.

The tasks to reach the goal are:

- Investigate possible causes behind abnormal hook load signal from literature and field data
- Make initial investigation to qualify the new hook load winch in the Institute for Petroleum Technology hall
- Plan, purchase and identify relevant equipment to build a new hook load rig.
- Build and develop hook model in laboratory for future use by master thesis and Ph.D. students at the Department of Petroleum Engineering and Applied Geophysics
    - Prepare the control unit to control the experiments
    - Develop procedures for hook load testing in lab
    - Simulate max tension during partly stuck pipe caused by cuttings jamming
    - Perform initial tests to verify the apparatus, the set-up, control unit and program for signals variation registration

2 Hook Load

Hook load is the sum of all forces acting on the drillstring suspended from the hook (Schlumberger, 2014).

Hook load measurements give a description of the weight of the drillstring and forces in the borehole. Changes outside of the expected values can indicate an alteration in downhole conditions. A description of the expected hook load is important for identifying any anomalies.

In order to develop an understanding for hook load measurements, a definition and an introduction to the relevant parameters make up the following section.

2.1 Hook Load Hoisting System

Historically the tension line measured the hook load weight. An accepted industry standard is to measure the hook load, W, as the tension in the deadline multiplied by the number lines in the blocks, N.

$$W = F_{dl} * N \tag{1}$$

This formula does not consider the sheave friction and does not separate between static and dynamic conditions (Fazaelizadeh et al., 2010).

Figures 1 and 2 below shows a complete setup of a hook load hoisting system. The tension meter is placed in the tesion line.

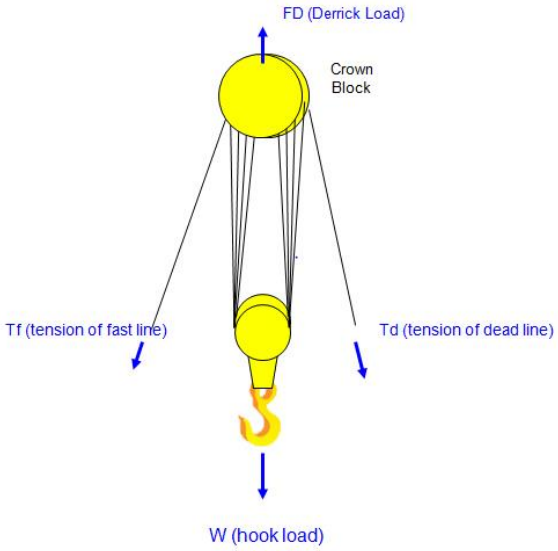

Figure 1: Detailed hook load set-up on rig.

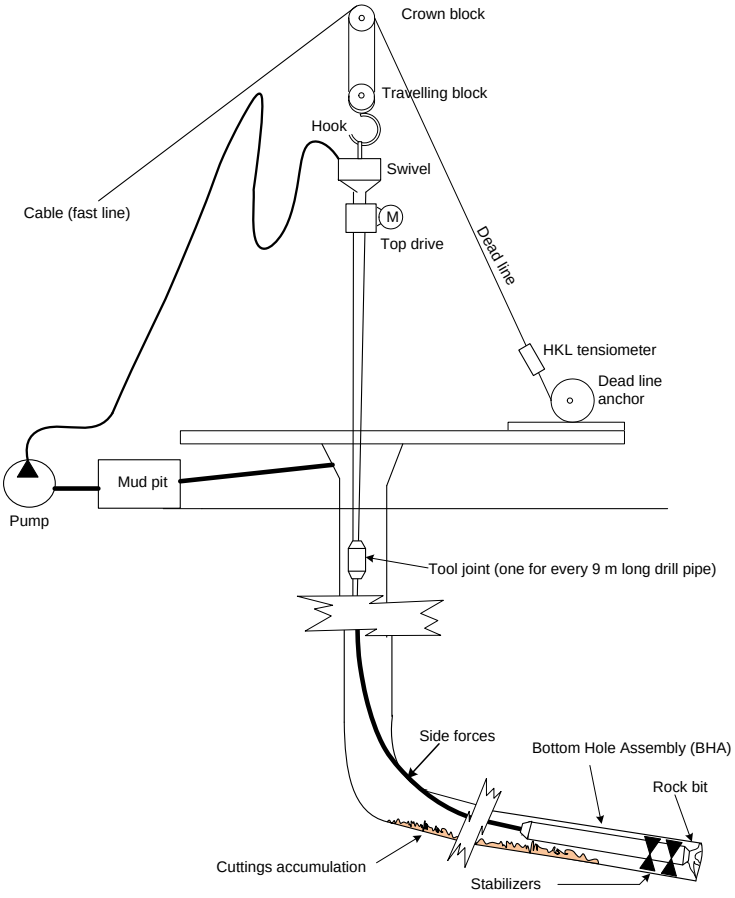

Figure 2: A rig set -up showing how hook load is measured (Skalle & Johanssen, Unpublished).

2.2 Modern Hoisting systems

In addition to the conventional winch and wire hoisting system, some new generation offshore rigs use hydraulic cylinders instead of the standard system described above (Aker Solutions, 2013). This concept is known as a RamRig™, illustrated in figure 3. Drilling equipment manufacturers such as NOV and Aker Solutions/ DRT offer this concept on their new constructions. This eliminates the need for drawworks and the traditional derricks.

Figure 3: Modern Hydraulic Ram Rig. Here the rig Aker Spitsbergen (Aker Solutions, 2013).

This new setup has advantages topside. It allows for safer and easier operations and frees up more room on the drillfloor. In addition, the system lends itself to exceptional (active) heave compensation and thereby control of toolface position relative to the borehole. However, there are downsides such as need for complex and large hydraulic systems, a rather narrow spacing around the rotary table and it is also more costly than a conventional system.

On these designs, the tension line is removed and the hydraulic cylinders measure the hook load. This removes some of the inaccuracies that the sheave block and lines cause due to added friction. The effect on hook load signal is minor as the vast majority of the weight comes from the drillstring and friction in the borehole. However, measurements that are more accurate can be

expected since the tension and deadline provide inaccurate measurements (Luke & Juvkam-Wold, 1993). This eliminates some of the uncertainties regarding the inaccurate measurements that the tension line and dead line show.

3 Physical Parameters Effecting Hook Load Measurements

The hook load varies when tripping downhole. Depending on the direction, angel and environment, the hook load registered topside can be very different for the expected value. These variations can cause problems, but also give valuable insight the downhole conditions if analyzed correctly.

The external forces that effect the hook load in addition to the weight of the drillstring are important to include when performing hook load analysis. The problems detected by hook load analysis are often diagnostic in nature. This means that it is a very good tool to help find the root cause of a problem after it has taken place.

The following chapter gives a description of the forces that effect the drillstring. Problems that can be detected by hook load analysis are also described and an explanation of how they can be relevant in detection and preventing downhole problems.

3.1 Drillstring weight and buoyancy

The traditional way of looking at a drillstring is dividing it into two components, the drill pipe and the BHA. The drillpipe is comprised of a steel pipe, traditionally in the 4-6 inch in diameter range and makes up most of the drillstring.

The BHA is located at the bottom of the drillstring and has a larger diameter then the drillpipe. It consists of equipment deemed necessary for the drilling operation and can vary in both size and content. The main objectives for the BHA are to:

- Protect the drillpipe from excessive bending and torsional load
- Control direction and inclination of borehole
- Reduce doglegs, keysets and ledges
- Increase bit performance
- Reduce string vibrations

- Contain MWD/LWD equipment

A typical BHA has a drillbit located at the bottom followed by drill collars, MWD/LWD equipment and stabilizers. Figure 4 shows the possible components of a BHA.

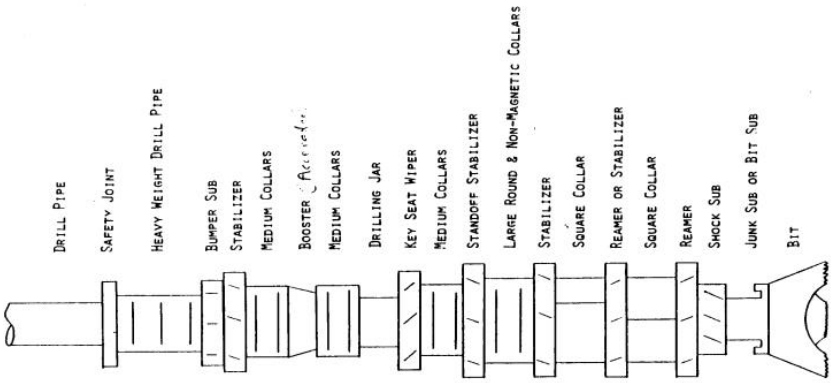

Figure 4: Showing a BHA with typical components (Aadnoy & Davy, 2010).

The drillstring is submerged in drilling fluids in the borehole. The fluids are commonly referred to as drilling mud. The fluid provides buoyancy, lifts the drillstring, and is a large factor when calculating the weight of the drillstring. The density of the mud compared to the density of the steel in the drillstring determines the buoyancy the mud provides.

$$\beta = 1 - \frac{\rho_m}{\rho_s} \tag{2}$$

The density of the mud is a factor when determining the design of the drillstring and particularly the BHA. In addition, in hook load calculations the buoyancy on the pipe has to be taken into the consideration. The contribution from the fluid, act as an upward force, making the total downward force less in a tripping situation (Sangesland, 2011).

The hook load registers the complete weight of the drillstring and BHA. The weight of the complete drillstring and BHA can be characterized by the following equation.

$$w = \beta * m * g * \Delta L \tag{3}$$

3.2 Friction

One of the most limiting factors in ERD drilling is friction. Friction is the force between surfaces in contact that resist the relative tangential motion. Tangential motion is defined as the sliding behavior between two surfaces and acts the opposite way of relative motion.

The most basic friction theory is the Coulomb friction. The forces action on a drillstring are shown in Figure 5 below. When sliding or pulling along an inclined plane, different forces are acting on the drillstring, depending on the direction of movement.

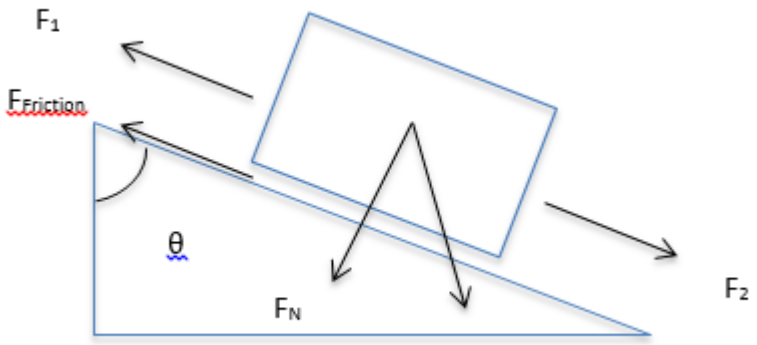

Figure 5: Forces in a straight borehole section.

Upwards or downwards axial friction form the borehole is defined as (Sangesland, 2011):

$$F_{Friction} = \mu mgsin(\theta) \tag{4}$$

When pulling the drillstring along a plane the contact between the forces can be described as:

$$F = mgcos(\theta) + \mu mgsin(\theta) \tag{5}$$

If the goal is to advance with the drillstring downward the borehole wall, the friction act negative to the movement, hence it has to be exceeded by the weight or additional downward force acting on the string, e.g. heavy drillcollars. The equation changes to (Sangesland, 2011):

$$F = mgcos(\theta) - \mu mgsin(\theta) \quad (6)$$

As mentioned earlier, friction is resistance against movement. During drilling, nearly all frictional changes come from axial friction that contributes to drag and torsional friction that contributes to torque (Sangesland, 2011). When tripping in or out of the borehole the hook load is primarily effected by axial friction. Resistance to rotational movement is defined as torsional friction. It can be derived from the speed of the string in the axial and rotation motion shown in Figure 6.

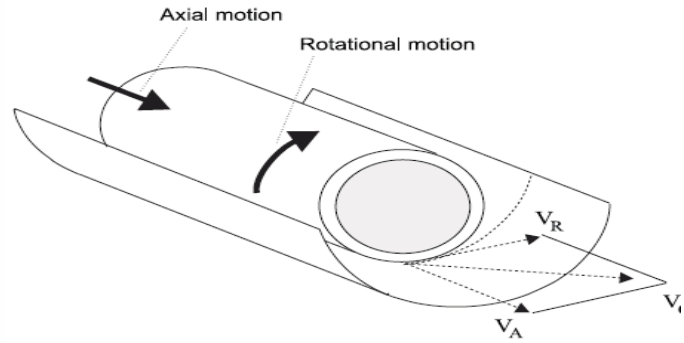

Figure 6: Axial and rotational movement in the borehole (Sangesland, 2011).

The axial movement V_A and the rotational movement V_R combined with the sliding friction derived above, makes up for the total friction acting on the string shown in equation 7 (Sangesland, 2011). When calculation torque is rotational movement always looked upon as a positive contribution.

$$F_{axialfriction} = \mu mgsin(\theta) * \frac{V_a}{\sqrt{{V_a}^2 + {V_r}^2}} \quad (7)$$

3.2.1 Torque and drag derivation

The definition of drag is the incremental force, which is required to move the pipe up or down in the hole (Johansic & Friesen, 1984). Drag is measured as the difference between the static weight of the drillpipe and the weight of the string when tripping (Aarrestad & Blikra, 1994). Depending on the direction of movement, drag might be positive or negative, as the derivation in the previous section illustrates.

The well trajectory and conditions in the hole influence the drag. In a vertical well, the well will support the drillstring weight, causing a reduction in drag compared to a horizontal well. An essential part of the drag calculations is to ensure sufficient weight on bit when drilling long horizontal sections.

Rotating the string when tripping in and out can help decrease the drag forces. Rotational movement of the string decreases the friction in the well, causing an overall reduction in the drag. Reduction of compression in the string is important to hinder critical buckling and stuck pipe.

When calculating torque and drag, different parameters are taken into consideration. In a smooth wellbore, different models are applicable dependent on the assumptions made in the analysis. However, in a true drilling situation the wellbore is seldom smooth. In order to account for the changes in inclination and azimuth, most computer program utilize the discreet model in a torque and drag analyzes (Sangesland, 2011). Calculating T&D by the discreet model, the drillstring is divided into different sections to account for the different contributions in the different sections. A curved hole section will increase the friction forces acting on the string, hence the torque and drag will enhance. By starting at the bottom and add up the different torque contribution throughout the string, it is possible to calculate the torque and drag at any point in the string.

3.2.2 Straight hole section

The discreet model for drag force in a straight borehole section is defined below and is defined in the same way as in the introduction to friction:

$$F_2 = F_1 + w * (cos\theta \pm \mu sin\theta) \quad (8)$$

As in the friction theory, is the friction acting negative while tripping into hole and positive when tripping out of the hole.

3.2.3 Curved hole section

For a curved borehole section the normal forces action on the string have to be modified to account for azimuth and inclination differences. The normal forces are altered by the wellbore and friction will increase from the straight hole. In Figure 5 an explanation of the following derivations is shown.

To account for the curved hole the drag forces changes to (Sangesland, 2011):

$$F_2 = F_1 + w * cos\bar{\theta} \pm \mu * N \quad (9)$$

+ = pulling the pipe

- = lowering the pipe

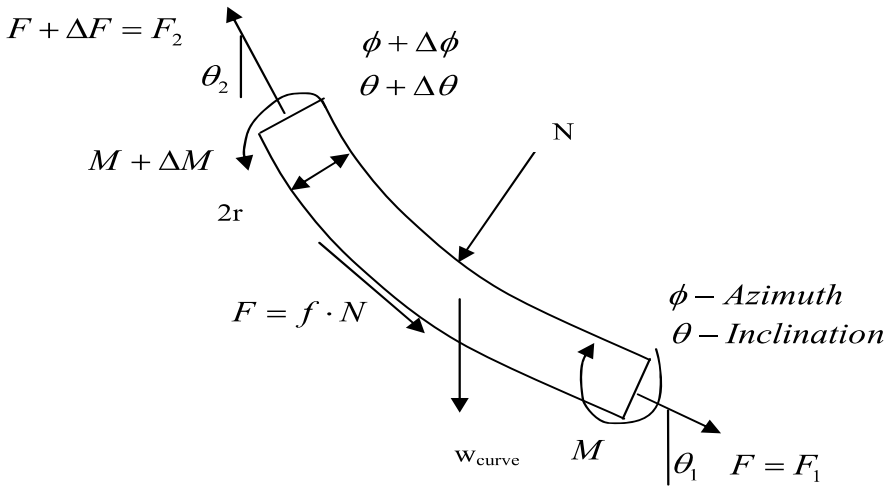

Figure 7: Discreet model of torque and drag (Sangesland, 2011).

The main difference from the straight hole section is the contribution from the wall on the string. The normal force accounts for both azimuth and inclination changes on one segment of the bit derived from the following equations:

$$N = \sqrt{(F_1 * \Delta\phi sin\bar{\theta})^2 + (w * sin\bar{\theta} + F_1 * \Delta\theta)^2} \quad (10)$$

$\Delta\phi = \Phi_2 - \Phi_1$ = Change in azimuth (radian) (11)

$\Delta\theta = \theta_2 - \theta_1$ = Change in inclination (degree) (12)

$$\bar{\theta} = \frac{\theta_2 + \theta_1}{2} \quad (12)$$

3.2.4 Coefficient of Friction (CoF)

When deriving the torque and drag equations above, the friction factor (μ) has to be incremented as a constant. The coefficient of friction factor (CoF) is often looked upon as the roughness between the borehole and the string. CoF is a dimensionless scalar value that describes the force required to move an object.

When tripping, the friction coefficient should be looked upon as a fudge factor. By including more than the mechanical contribution, a more accurate estimate of the friction coefficient is calculated. The friction coefficient comprises of:

- The stiffness of the pipe
- The resistance from the fluid on the pipe movement (viscous drag)
- Obstructions in the wellbore and stability related problems.
- Formation type, variation in lubricity
- Pore pressure
- Micro - tortuosity

The CoF is not a function of the mass or volume of the objects involved. Only the type of material and contact between the materials affect the value. The CoF reflects the behavior as seen in static and kinetic friction. Static friction is the friction force between two objects when there is no relative movement between them. Once an object starts moving it will overcome the static friction and becomes kinetic friction. As long as an object is standing still, the static friction will be equal to the applied force. When the object starts moving the friction will drop when it becomes kinetic. This is based on the concept that it takes more applied force to start movement then to keep it constant. When two surfaces are moving relative to each other at low speeds, the kinetic friction is almost constant. The roughness of the contact surfaces dominate the force of friction. Figure 8 illustrates the static and kinetic friction vs. time.

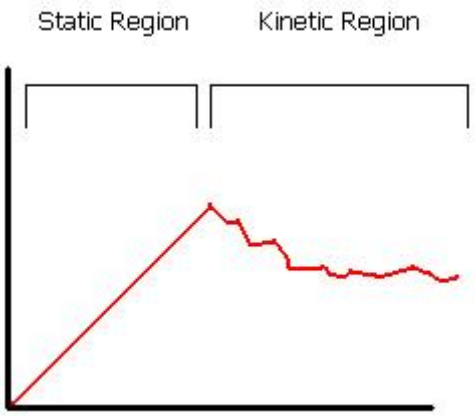

Figure 8: Static friction and kinetic friction as a factor of applied force (Townsend, 2002).

The phenomenon of static vs kinetic friction is often very visible in hook load curves and will be shown in the later sections.

Examination and analyzes of the friction coefficient hence the resulting torque and drag creates a more accurate picture of the well stability and the formation which are/where drilled. The CoF is often the limiting factor in drilling ERD and is an important factor during both drilling and tripping operations.

During tripping, the CoF represents all the factors in the well that add to the hook load except for the weight of the drillstring, as eq.13 shows.

$$HKL = \Sigma\,(w * cos\theta \pm \mu * F_n) \tag{14}$$

The CoF will vary in the borehole due to the changing conditions. In addition, the friction can never be truly be known before an actual observation is made during tripping or drilling.

3.3 Fluid Drag

When pulling an object through a fluid, a friction occurs from the contact between the surface of the object and the fluid. This is known as fluid drag. When pulling the drillstring, the mud exerts an extra friction. The amount of fluid drag exerted on the drillstring will depend on the relative velocity between the two objects, as well as the viscosity of the fluid. The viscosity of the fluid will have a greater impact on the amount of drag then the velocity (Polak & Lasheen, 2002). Fluid drag can be expressed as follows:

$$F_{D=}\frac{\pi d_s \mu v L}{D_{h-D_s}} \tag{15}$$

Where

- F_D is fluid drag
- D_s and D_h are diameter of drillstring and hole respectively
- L is the length of contact
- v is the relative velocity between the objects
- μ is the fluid viscosity

The CoF will no longer include fluid drag when it can be calculated or assumed. The CoF in a calculation including fluid drag will be the friction between the borehole and the drillstring only.

3.4 Elalstic behavior

While tripping the drillstring experiences a compression or tension force. The force might cause the drillstring to deform. This may effect the hook load weight and the depth measurement of the drillbit. A drillstring is as an elastic object. The definition of elastic behavior is a deformation that is not permanent. When the tension or compression force is removed the object returns to its original state. In figure 9 we see the stress vs strain curve.

The elasticity of an object depends on the properties of the material. Young Modulus is the standard method for describing elastic behavior.

$$\sigma = \frac{F}{A_{cs}} \tag{16}$$

$$\varepsilon = \frac{\Delta L}{L} \tag{17}$$

$$E = \frac{\sigma}{\varepsilon} \tag{18}$$

Where

-σ is the symbol for stress

-A_{cs} is the area cross section

-ε is the strain

-F is applied force and

-L is the initial length and E is the Young modulus.

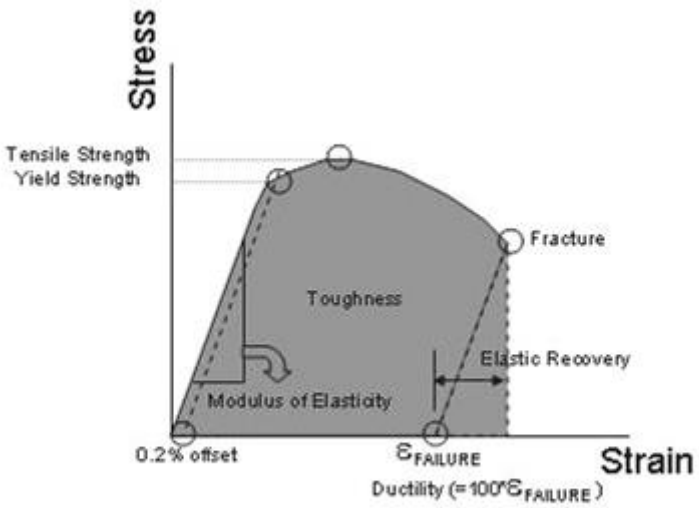

Figure 9: Stress vs strain curve (Etomica,2014).

By substituting the equations into eq.19 the length of deformation can be derived from the equation:

$$\Delta L = \frac{F * L}{E * A_{cs}} \tag{19}$$

This equation gives the resulting stretching of the pipe and change in borehole length. This is provided the stretching does not surpass the yield strength, which would result in a permanent deformation.

4 Hook Load Signatures during Tripping From Literature and RTDD

In order to asses if the laboratory model was built correctly, the hook load signatures recorded in the laboratory have to resemble real life data. To achieve this, a study of normal tripping curves through RTDD and study of literature on the subject was conducted. When a norm was established, different borehole problems were looked at and a signature identified. The RTDD was pulled from the Gullfaks Well 34/10-C-47.

Well 34/10-C-47 was spudded on the 25.11.2005 and finished completed 25.04.2006 at Gullfaks C. The cost of the drilling operation was estimated to be 191 million NOK. During the process the 17 ½" and 12 ¼" section were the two most challenging sections. Drilling costs were budgeted at 110 million NOK. Due to the well problems encountered the operation eclipsed the budgeted time by 63,1 days. The finished operation exceeded the budgeted cost by 81 million NOK, ending at 191 million NOK.

The most severe cases of NPT came in the 17 ½" section and 12 ¼" MPD section. 96 hours were spent POOH in the 17 ½" section after finding indications of pack off and after the first run in the 12 ¼" section a total of 11 days passed until the next run due to lost circulation.

Table 1: Planned vs actual drilling operation times ref. (Statoil, 2007).

Section	Start Time	Budget		Actual		Operational Time (%)
		Hrs	Days	Hrs	Days	
Prespud	25.11.2005 15:00	44,5	1,9	78,5	3,3	96,6
24"	28.11.2005 21:30	319,1	13,3	575	24	90,6
17 1/2"	22.12.2005 21:00	638,8	26,6	795,3	33,1	71
12 1/4" MPD	27.01.2006 15:15	231,1	9,6	694,3	28,9	72,5
8 1/2"	25.02.2005 14:00	362,7	15,1	303,5	32,5	96
Sum		**1596,2**	**66,5**	**2446,6**	**121,8**	**85,34**

The 17 ½ section was drilled utilizing a relative constant inclination of 60 degrees. Small changes in the azimuth and inclination were necessary due encountering unexpected geology and faults. Problems encountered during drilling led to increased tortuosity, especially in the 17 ½" section,

which increased the dog leg in the well. An illustration of the end wellpath smoothness is shown in Figure 9. The end wellpath shows a slight deviation from the planned wellpath.

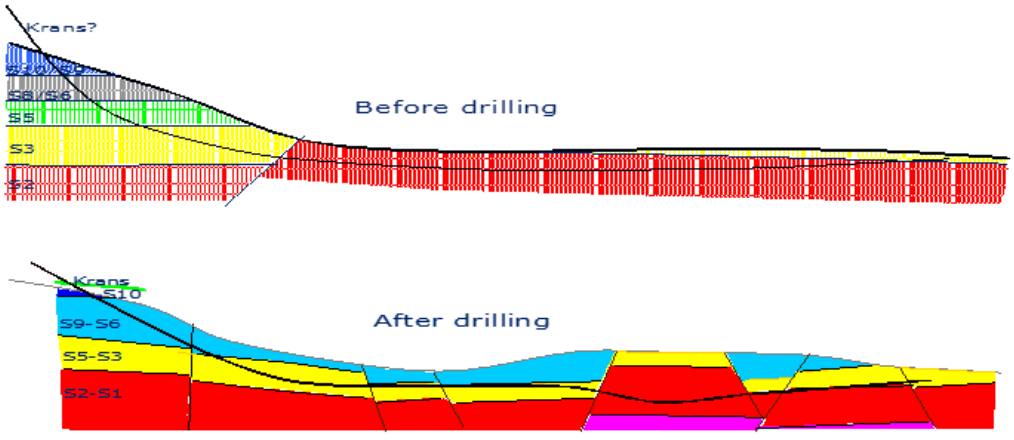

Figure 10: Planned vs actual wellpath (Statoil, 2007).

The 17 ½" section was drilled from 1515 m MD using 3 runs and TD was reached at 2379 m MD. During these runs, the most common problems were related to stringers and erratic torque behavior. The first drilling run in this section was particularly troublesome. This run was drilled from 1515,5 m to 2070 m MD and reaming was necessary underway to keep drillstring from stalling. A new type of mud, Ultradrill, which had not been previously used in Statoil wells was used. The ultradrill drilling mud consisted of WBM with added synthetics that caused problems in this section. The End of Well report lists this as reason for the sticky cuttings in the shale formation. The next drilling run was drilled using another mud and no problems of the same magnitude were encountered, despite drilling in the same formation.

When it was decided to POOH pack off, symptoms were observed and several days were spent reestablishing desired circulation and reaming the hole. A total of 96 hours NPT were registered before the drillstring was POOH and the problem section cleared. The End of Well report lists symptoms of packing off as the reason for the trouble POOH.

A MatLab code designed by Mme was used to extract the RTDD data supplied by Statoil. When extracted to excel and analyzed in a program called DrillEdge. DrillEdge is a program developed by Verdande Technology for recognizing events during real-time drilling.

4.1 Normal Hook Load during Tripping

When tripping the RTDD presents the hook load along with the block position. During drilling, a drillstring connection is conducted approximately every 30 meters (90 feet). Each one of these sections of the drillstring are referred to as stands. When a stand is made up and attached to a new one, it is referred to as a connection. Figure 11 illustrates a drill floor with the block raised and ready to make a connection. The protuberance on the drillstring are the tool joints. These are where each connection is made.

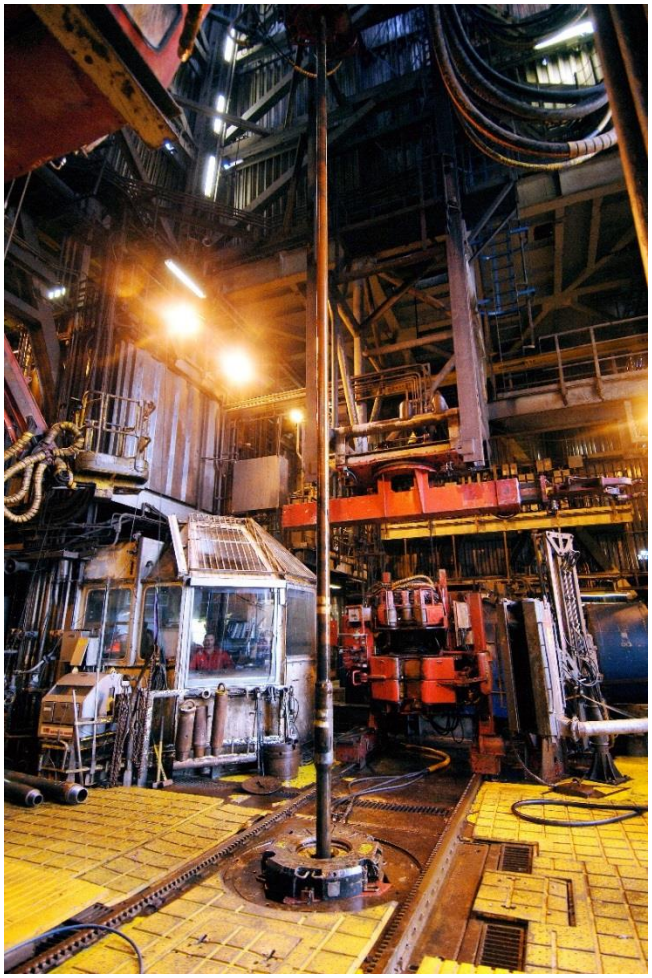

Figure 11: Drillfloor with traveling block hoisted and ready to disconnect a stand (Wikipedia, 2014).

In order to identify an expected hook load signal a norm has to be established. When the block hoists the drillstring the tension in the tension line increases. The pipe will start to move once the static friction is over won. The initial friction to start the movement means the hook load has a sharp increase followed by a "top". Once the drillstring starts moving, kinetic friction takes over and a small decrease hook load as the block moves upward, as shown in figure 12 (Cordoso Jr et al., 1995).

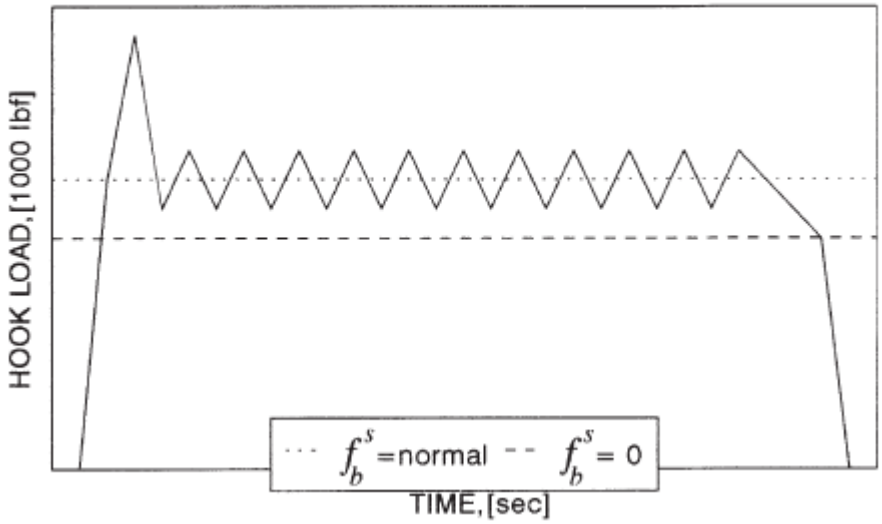

Figure 12: From study by Cordoso et, al. indicating a normal hook load reading for one stand (Cordoso Jr et al., 1995)

From the RTDD data figure 13 shows normal tripping curve of one stand. The hook load curve nicely resembles the hook load curve in figure 12. The features of a normal POOH can be easily recognized.

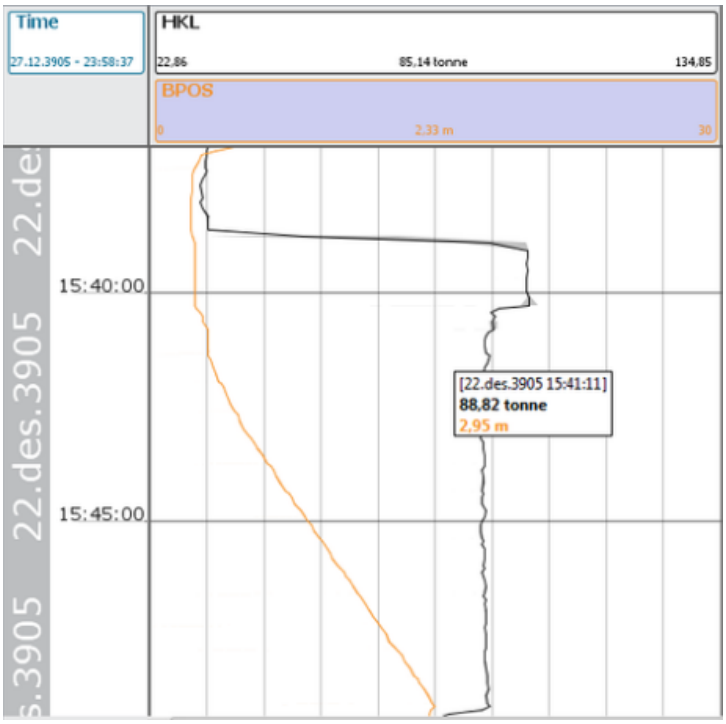

Figure 13: Normal hook load curve during POOH from RTDD data

4.2 Abnormal Hook Load readings

An abnormal hook load signal will be one that deviates from the expected trend. During tripping these will usually show up on the RTDD as an overpull. Overpull is when the drillstring is being POOH and the weight indicated on the tension line exceeds the expected and calculated hook load. This section presents several hole stability issues which can be detected on the hook load. A focus on this section will be pack offs and cuttings accumulation.

4.2.1 Pack Offs

Pack offs indicate that the borehole is having stability issues. In addition to the increasing hook load, it will also be recognizable by an increase in pump pressure or standpipe pressure while the mudflow into the well is constant (Shokouhi et. al, 2009). Pack offs can be caused by a number of different issues.

The most common pack off is when the formation collects around the BHA and bit. This is known as cuttings plowing, illustrated in figure 14. Cuttings plowing is particularly an issue in deviated wells with an angel between 30 degrees and 65 degrees (K & M Technology, 2011). The angel of the well causes the cuttings to avalanche and collect around the BHA. This problem is often not detected until the drillstring is POOH. The bit and the BHA cause a shoveling effect. This causes the cuttings still in the borehole to accumulate and eventually restrict movement of the entire drillstring.

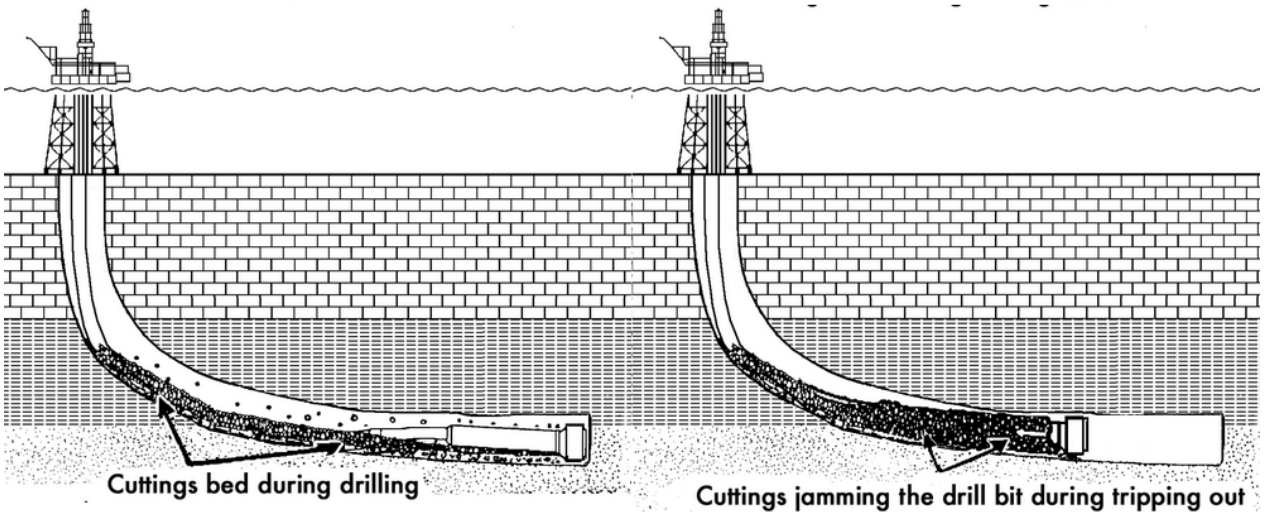

Figure 14: Cuttings jamming during tripping (PetroWiki, 2014)

The reason for cuttings collecting around the BHA are numerous. Most are a result of improper hole cleaning. This will occur if the cuttings transport is insufficient. Aside from creating hydrostatic pressure, one of the main objectives of the drilling mud is to function as a conveyer belt for the cuttings. The mudflow will carry the cuttings to the surface.

Another common reason is a result of the hole caving in higher in the borehole. This causes the cavings to collect around the BHA. Shale swelling is also considered a pack off. It is recognizable by many of same symptoms as poor cuttings transport. The shale swells when in contact with the drilling mud causing it to wrap around the drillstring or BHA causing a restriction in flow in annulus.

If no action is taken when experiencing a pack off, it can result in a mechanical stuck pipe incident. This means that the drillstring is not able to move in the borehole. Maintaining a proper RPM of the drillstring is vial in reducing pack offs. The rotational movement of the drillstring lifts the cuttings into the path of the flowing mud in the annulus and transported to the surface. Other remedies against pack offs can be changing the rheology of the mud, circulating the hole clean and bull heading.

Pack offs will be recognizable on the RTDD as increase in hook load and growing pressure in the standpipe. The mudflow into the well will be constant but the cuttings will form a restriction on the flow in the borehole, causing the pressure to build.

For packoffs it is difficult to free the pipe without resorting to back-off methods. To back off implies freeing the pipe by severing it at a certain point. Backing off will leave drillstring and BHA in the hole. It is possible to fish these out of the hole, but in many situations the it will result in lost BHA. Potentially resulting in several millions kroners in lost material and equipment. In It is therefore imperative to reduce the number back offs during drilling operations.

4.2.1.1 Overpull while POOH

Date	26.12.2005	27.12.2005
Time	00:00:00	23:59:00
Measured Depth (m)	2070	1673

Drilling continued until 2070 mMD where the power drive failed to turn and the decision was taken to POOH. The failure of the tool was most likely a result of previous problems in the well. The hole was circulated BU x4 before the End of Well report suggests symptoms off packing off

were noticed. Minor mudloss events and mild breakover drag events were the only events with a large time span between these events. The End of Well report suggested that there was a severe overpull event of 15 tonnes on the 27. December. The event has been found and highlighted in figure 15.

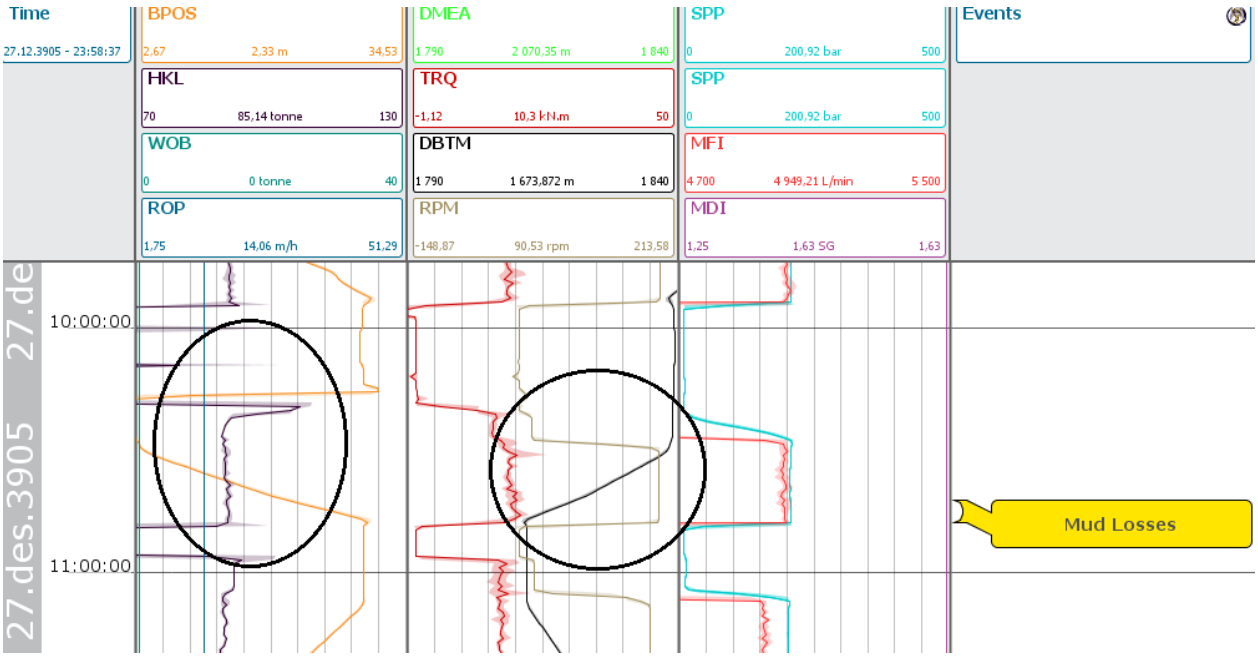

Figure 15: Overpull event from RTDD

The mud loss events were most likely an effect of the Utradrill mud which cased poor hole cleaning. The End of Well report suggested that cuttings were left in the borehole with the mud sticking to the cuttings which could cause the volume of the active tank to drop.

4.2.1.2 Erratic Hook Load and SPP increase

Date	24.12.2005	24.12.2005
Time	13:00:00	22:10:00
Measured Depth (m)	1885	1945

After the previous problem where the overpull was registered drilling continued with reaming being necessary on a number of occasions. Symptoms of pack off are present and it is obvious that the drilling crew has been aware of these signs.

From 11:00 to 12:10 the SPP increased from 182 bar to 188,89 bar despite MFI being stable at around 5000 liter/min. Figure 16 shows the steady increase in SPP while the MFI is constant. This is a strong indication that the mud flow was facing restrictions downhole and had troubles circulating in the annulus. No event is fired in this time space.

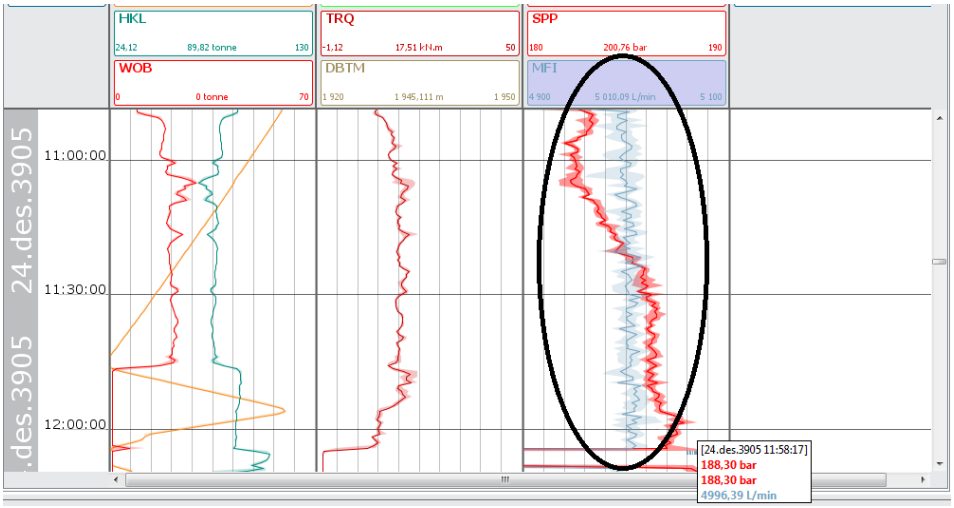

Figure 16: Increasing SPP indicating downhole restriction of flow

The trend of small, but yet noticeable SPP increases along with erratic torque continued, with the drill crew seemingly aware of the risks. Reaming and circulation was initiated after each SPP increase.

At 21:40 the MFI in was increased from the normal 5020 L/min to 5200 L/min while circulating, as seen in figure 17, presumably to improve hole cleaning. When the bit reached bottom the MFI was again reduced to 5020 L/min while an increase trend in SPP was again noticeable. The bit was again lifted off bottom and an increase in hook load above the expected trend was noticed along with very erratic torque behavior. The drillstring at this point stalls along with high breakover torque.

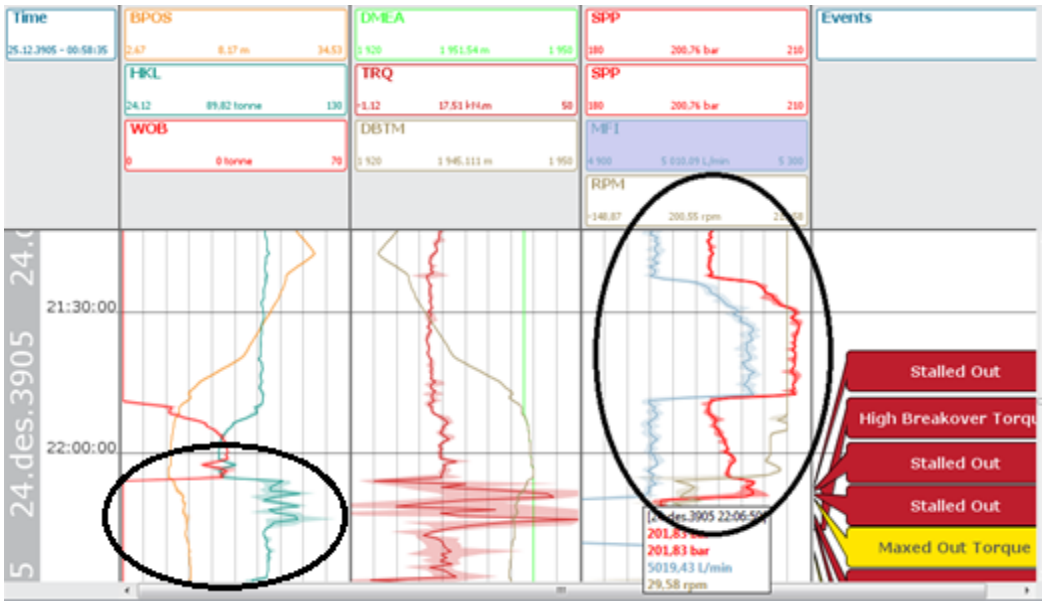

Figure 17: Increase in SPP and erratic hook load curve when hoisting drillstring

The stalling out and erratic torque can be seen as consequenses of the hole partialy packing off. Raisng of the drillstring is indicated floowed by a sharp increase in hook load. It is clear that the reason the bit was pulled off bottom was the increase in SPP. The large pressure increase directly in advance, which was a result of the MFI being increased to 5200 L/min, could result in the SPP increase at 5020 L/min..

Another explantion could be that the drill crew were be alert in this section and immediately took action when a increase trend in SPP, torque or hookload was seen. Every time an abnormal increase in SPP was registerd the bit was pulled off bottom and reaming and circulation was initiated.

4.2.2 Differential sticking

During drilling, the hydrostatic mud pressure must balance the pore pressure in the borehole to prevent fluids from entering the well. In a permeable zone, the mud will infiltrate the formation. The solids in the mud will collect on the wall of the borehole, forming what is known as a filter

cake. If a filter cake grows sufficiently large, the drillstring or BHA may become embedded against the borehole wall. The differential pressure between the filter cake and the borehole pressure causes the drillstring to be stuck. When the drillstring is pressed against the side of the borehole, it will still allow for full mudflow. Therefore, a differential stuck pipe can be recognized on the RTDD as a sharp increase in hook load and an expected mudflow.

Eq.19 expresses the force necessary to free a differential stuck pipe

$$F = \Delta p * A_c * f \tag{20}$$

Where the different parameters are shown in figure 18.

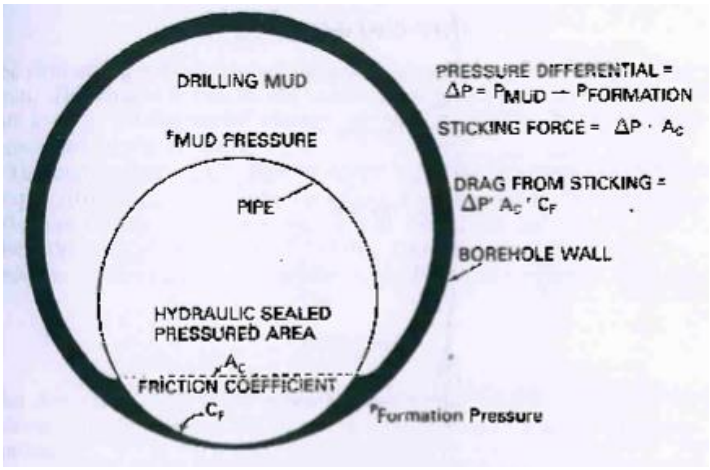

Figure 18: Differential sticking (Aadnoy & Davy, 2010)

Differential sticking is particularly a problem in deviated and horizontal wells, since the drillstring will drag against the low side of the well (Aadnoy & Davy, 2010). The risk of differential sticking also increases when the drillstring is static. Figure 19 shows a signature curve for differential sticking.

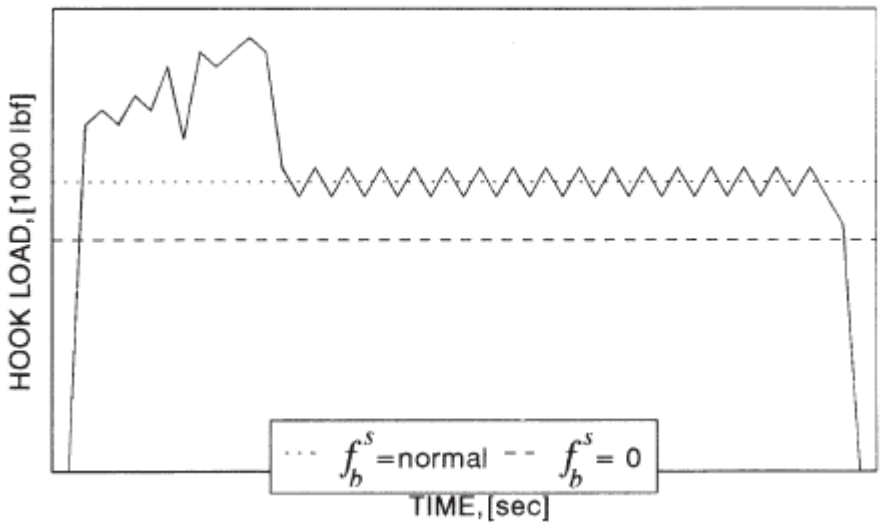

Figure 19: Hook load curve indicating differential sticking (Cordoso Jr et. al, 1995)

Gullfaks-34/10-C-47 well contained no differential sticking events. Therefore, no signatures from RTDD are presented in this thesis.

4.2.3 Key seat, ledges and or dog leg

An abrupt change in hole angle or direction that causes a sharp bend in the wellpath is known as dog-leg. It can be detected by an increase in torque and hook load readings. The dog leg can be calculated using the suvery results over an interval of about one stand or 30 meters.

$$\varphi = \cos^{-1}[\cos\alpha_1 * \cos\alpha_2 + \sin\alpha_1 * \sin\alpha_2 \cos(\beta_2 - \beta_1)] \quad (21)$$

Where:

-φ is the dog-leg

-α is the inclination

-β is the azimuth

When expressing dog-leg it is usually given as change in angle per 100ft drilled. This is called Dog-leg severity (DLS) and can be expressed as:

$$DLS = \frac{\varphi}{L} * 100 \quad (22)$$

Where:

-DLS is degrees per 100 ft.

-L is length between survey points in equation 21.

A key seat will occur as a result of drilling in a section with dog-leg. Key seat is particularly a problem related to POOH. When drilling the drill pipe is kept in tension. When the drillpipe passes through a dog-leg, the tension will force the it against the wall. The continued rotation during drilling means the drillpipe "eats" into the formation causing a groove. See figure 13.

The problem occurs when tripping out of the borehole. The drillpipe may pass through the grooves it has created, but when an object with a larger diameter, such as tool joints or BHA, they will become stuck. The pipe can be lowered and rotated but is unable to move upwards.

The solution is to commence a reaming operation. The drillstring is usually equipped with spiral stabilizer or key seat wipers. These are blades the are attached to the upper part of the BHA. The pipe hrotates and moves up and down along the problem area. The cycle is repeated until the key seat has been reamed out and the drillstring can now pass through (Aadnoy & Davy, 2010).

In figure 20 a typical hook load reading when the drillstring is caught on a ledge or key seat.

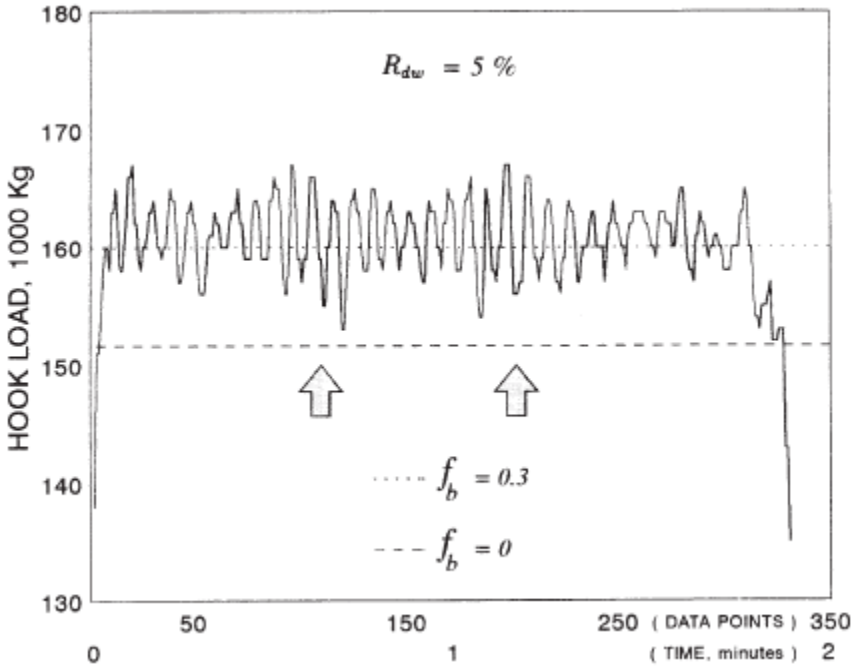

Figure 20: Indication of ledge (Cordoso Jr et. al, 1995)

4.2.3.1 Key seat

Date	24.12.2005	24.12.2005
Time	04:30:00	06:10:00
Measured Depth (m)	1790	1820

At 1790 m MD to 1800 m MD there was a serious overpull event followed by a maxed out torque. Prior to this event the borehole had been drilled for about an hour after the hole had been reamed. The increase in WOB and decrease of hook load is most likely the reason reaming was deemed necessary again. The block position was raised and a large increase in hook load was registered, as highlighted in figure 16.

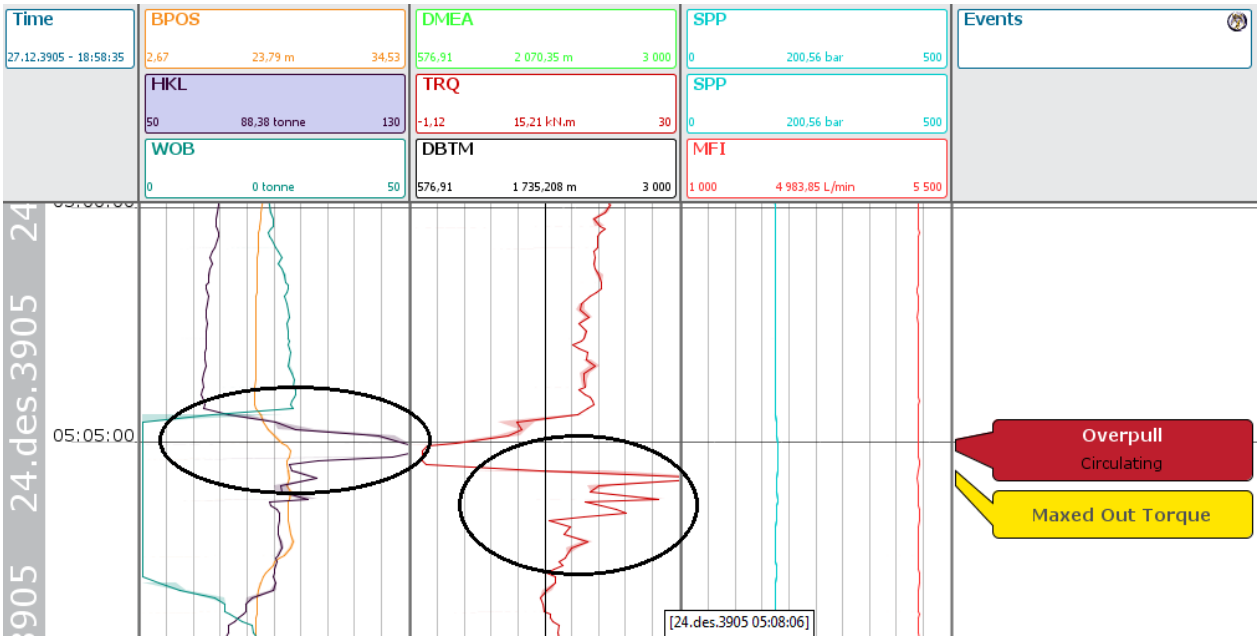

Figure 1: Showing overpull in time window in DrillEdge

The overpull has to be seen in connection with the problems which previously had occurred in the well. 15 minutes prior there had been 2 hard stringers encountered as shown in figure 16. Also the power driver on the BHA which was set to “hold inclination” had failed and struggled with communication. This could result in high local dogleg in the well, as was indicated in the survey data. The dogleg at 1824 m MD was recorded at 2,59 deg/30m (Sta071) which is a relatively high dogleg in this well. The BHA has a wide range of different OD’s making it more susceptible to being caught in the event of high doglegs and hard stringers. The BHA could easily have been caught on the hard stringers and resulted in overpull.

The steady trend of increased hook load could have been signs off packing off. However, the steady mud flow suggests that the pack off would not have been very severe. In case of a severe pack off there would be a sharp increase in the SPP as a result of the mud flow being restricted from flowing through the annulus. The increase in hook load was most likely the reason that the bit was pulled off bottom.

The overpull did not reoccur which indicates that the drillstring was pulled away from the obstacle it was caught on and that it was not a pack off. Figure 21 shows that no further action

was taken from the drilling crew and drilling was resumed immediately after. It was a reasonable conclusion that the BHA had been pulled clear of the restriction.

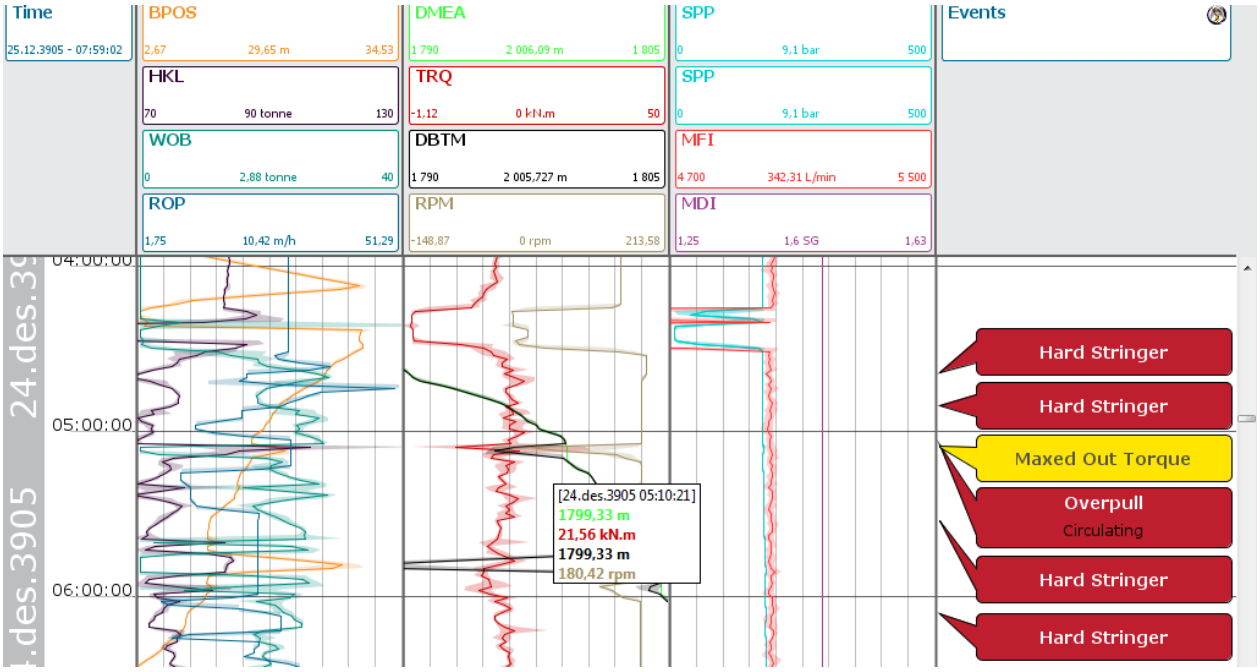

Figure 21: Longer time-view of the overpull event, showing hard stringers before and after.

In hindsight this was an indication of the problems that followed during further drilling the well. From this point on the well had an increasing amount of pack off symptoms.

5 Previous published literature on Hook Load Evaluation

This section will look at why recognizing signatures in drilling parameters is important and give a recap of hook load evaluation done at NTNU.

5.1 Monitoring of drilling parameters-The relevance of establishing symptom recognition models.

One of the major expenses is the non-productive time (NPT) related to drilling. With the increased challenges of drilling, NPT is a rising concern for the industry. During drilling NPT annually amounts to as much as 35% of the costs of the operation. With offshore rig day rates currently residing at an average of $ 429 806 USD/Day (Offshore.no, 2014) for floaters on Norwegian sector, it is evident that tools that contribute to reduction of NPT can save large expenses for oil companies.

Real time monitoring of drilling parameters has had a growing importance in drilling operations (Booth, 2011). Establishments of offsite locations, called Real Time Operations Centers (RTOC), is an increasing trend in order to optimize drilling operations and reduce NPT.

Real Time Operations Centers (RTOC) are the new and efficient way of aiding real time drilling operations. RTOCs experienced a comeback in the early 2000's after the 1980's RTOCs proved redundant and inefficient. The RTOCs of today have proved to be both reliable and cost saving. They improve HSE by demanding fewer personnel on board rigs and provide assistance and advice for personnel on location (Booth, 2011).

RTOCs work by having staff located offsite monitoring a number of operations at the same time. By analyzing the real time drilling operations people with expertise can observe the stream of data coming in from operations and help the often lesser experienced personnel on location. They can also have a longer perspective on time and identify patterns that on location personnel often fail to see or miss due to other tasks they perform.

These RTOC's provide valuable insight to an operation the onsite personnel might not have the capacity to monitor. It is in these environments that a hook load models and symptom recognition is relevant. In these settings, an established method for dealing with hook load symptoms would prove valuable and save operational costs as well as time.

5.2 Previous work on Hook Load at NTNU

Literature on hook load models and hook load signatures are scarce. This means that the work conducted at NTNU is even more important. There have been several attempts at modeling hook load, with varied success. A short summary of their finding is included in this paragraph. These have been important in building the hook load model. Their experiences have been taken into consideration in the planning, building and construction of the hook load laboratory setup. The basis of most hook load thesis have been a model developed by Mme. The mass-spring model was made to simulate normal hook load during tripping. Several students have made steps to qualify and improve the model through programming and hook load signature studies. However, the conclusion seems to be that the model is difficult to improve and provides very varying results during simulations. Figure 22 illustrates the principle behind the mass-spring model.

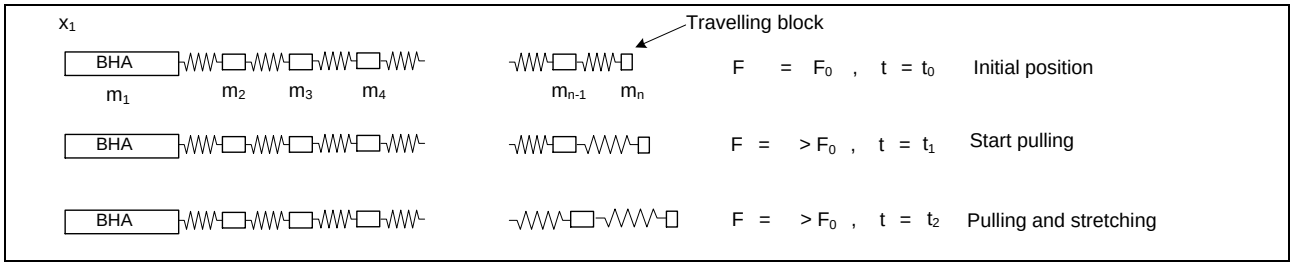

Figure 22: Mass-spring model and its response to being pulled (Skalle & Johanssen, Unpublished)

The model is based on that hook load acts as a spring during initial pulling. Due to the amount of work previously done on the model and the conclusions reached in their thesis, the model was not developed further in this thesis.

Edvin Kristensen (2013) attempted to develop the mathematical mass-spring model. The conclusion was that the model provided good results, but was very sensitive to changing conditions. In order to be a good tool for problem detection the model has to be further tested.

Tina Glomstad (2012) tested the mass-spring model on the previous hook load set-up in the labratory. Her conclusion was that it was difficult to conclude that the model provided accurate results. The laboratory set-up the model was tested on had been built by Det Norske. The experiences from working with this model is foundation of the development of the new hook load rig.

Some of the most important experiences from the previous hook load model:

- The positon of the drillstring was measured once every second. This proved to be insufficent.
- Unable to produce the initial peak during testing the labratory hook load model
- Velocity drops seems to match hook load peaks
- Lack of procedures and testing of model meant that the set-up was difficult and impractical to use during experiments and to recreate identical conditions for testing.

Hanne Bjerke (2013) studied RTDD data from a number of Statoil wells to find and identify problems that were detectable on hook load signatures. Figure 23 highlights the most important finding. It is a recognition of hook load signatures during various restrictions.

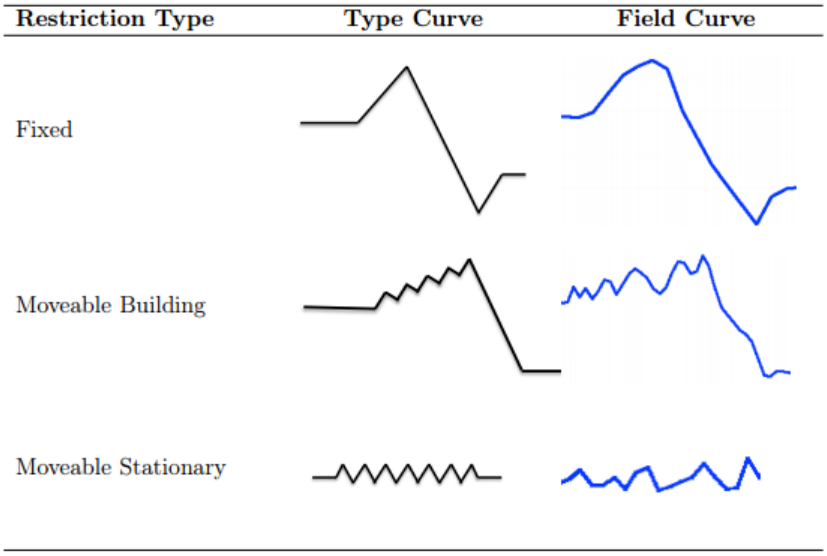

Figure 23: Hook load signatures while encountering restrictions during POOH

Figure 24 shows cuttings accumulation during POOH from RTDD. It is particularly relevant for this report has been included as an example of a standard cuttings accumulation signature.

The Hook load clearly increases as the drillstring is POOH indicating a restriction in the borehole. Because the drillstring is still moving it is a moveable restriction.

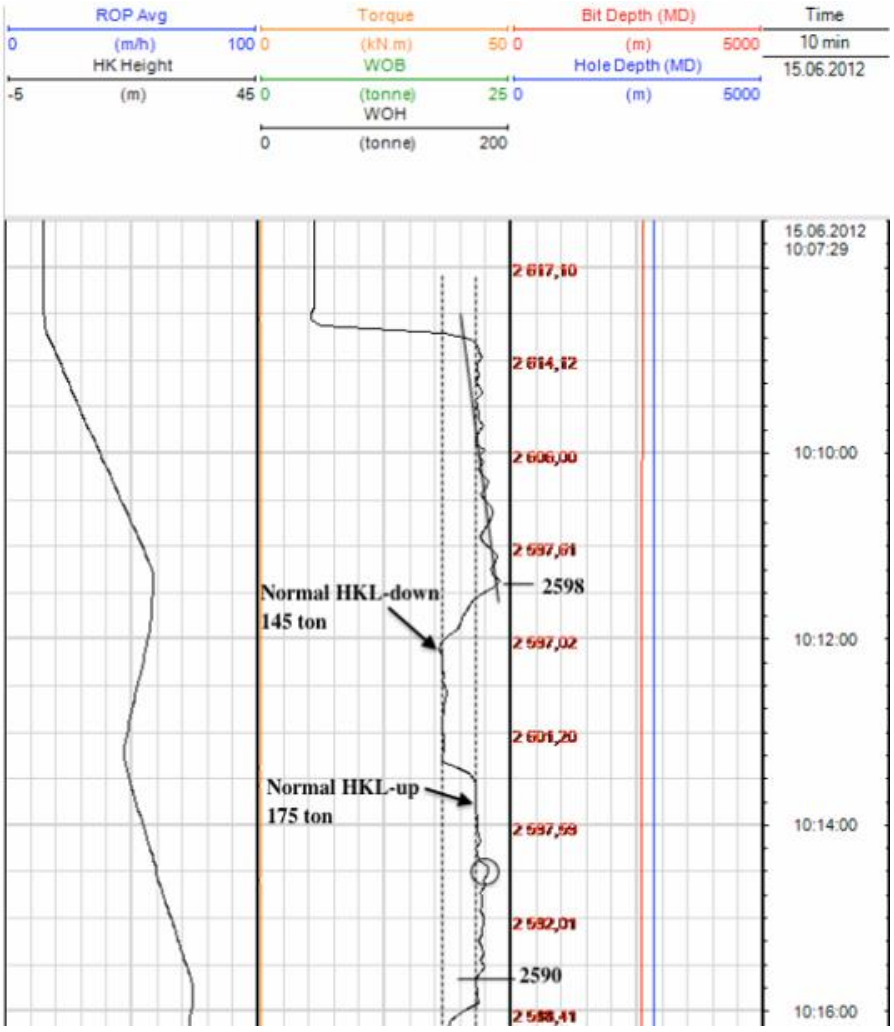

Figure 24: Cuttings accumulation in from RTDD data (Bjerke, 2013)

6 Hook Load Model Experiment

In order to better understand the forces acting on the drillstring and recognize patterns in hook load signals a scaled model and laboratory apparatus was built. The apparatus consisted of elements representing the drilling rig hoisting system, low-pressure mud circulation system, the drillstring including BHA, the borehole and relevant controls and instrumentation. The apparatus should be able to adequately simulate a stand being pulled out of hole for research and experiment purposes. In the IPT hall there was already an existing hook load set-up. Students have previously worked on this for various experiments and projects. However, as explained in the literature from chapter 5.2 regarding previous NTNU work, the experiment set-up had several flaws and proved to be too decrepit. The model and set-up was not able to conduct several of the desired experiments (Pål Skalle, 2014). It was therefore concluded at the outset of this thesis work that a completely new model/apparatus had to be constructed.

This new complete hook load rig was located at the laboratory at PTS. This rig is downscaled, but will have the most vital functions of a full-scale drilling rig. A number of research projects including Ph.D's are planned over the next years (2014-2017) regarding hook load models.

A new, stronger winch had already been sourced. Due to the increased pulling force of the new winch, none of the main components of the previous model could be re-used because the tension forces applied would have exceed the capabilities of the previous model. In addition, there were a number of other issues, listed in chapter 5.2. A sturdier and more robust hook load rig was designed and set-up instead. An advantage of creating hook load rig is that the data acquisition rate will be up to 1000 Hz or 1000 measurements/second. On field data the normal acquisition rate is 0,3 Hz or one measurement per 3 seconds.

This section will describe the different phases of creating the model and describe how it works. The LabVIEW section is intended to give persons working on the same model insight into analysis the readings and data from the laboratory set-up. In addition, it will provide a platform to develop hook load models for future work.

To reach the goals of the new rig, designing building and testing the hook load set-up were the main objectives of the master thesis. The build process will be described in detail in this section and the results of the testing will be presented in the next section.

6.1 Planning and execution summary

Several criteria were set before the building the hook load rig commenced. During the planning phase, the following principles were emphasized for the laboratory set-up:

- Robust
- Interchangeable
- Safe

Achieving the desired functionality was a focus early in the design process. During testing, the fixed objects that are probable to be changed need to be easily accessible. Due to the fact the previous set-up had to be completely replaced, care was taken to evaluate the shortcomings of the old rig and implement the required improvements on the new set-up. To avoid future users having to construct a completely new rig or perform time-consuming modifications, each part of the hook load laboratory set-up was made easily replaceable. The parts deemed necessary for easy replacement to efficiently achieve parameter variations during future testing and research work were:

- Pipe lengths representing the borehole
- Pipe diameter size (borehole ID)
- Drillstring and BHA composition

The main problem with the previous model was that it was not sturdy enough to support large loads. The new model's position was close to the ground in order to counter act the large tension forces. A model built with higher elevation would be at mercy of the strenuous forces it would have to endure. By placing the model at ground level, it allowed for both cost and material savings. For the foundation of the set-up, a large steel beam was placed at the center of the construction.

From the study of hook load literature and RTDD the most important parameters during hook load were identified. The following parameters were to be included in the experiment simulations:

- Hook Load (HLK)
- Block Position (BPOS)
- Velocity
- Fluid drag
- Fluid flow

The addition of the fluid flow parameter was because the study of signatures for cuttings accumulation revealed that flow was an important factor in recognizing stuck pipe situations.

For the initial testing, it was decided that a horizontal test pipe was sufficient. For a test with inclination to be possible, it is necessary with a few adjustments.

Because of the large loads the new rig will handle safety was an important aspect. When the winch is pulling several hundred kN of force, it is crucial to be able to closely monitor the forces and relieve any excessive stress when necessary. Both equipment and persons could potentially be harmed if the system is overstressed. In keeping with oil and gas industry practice, several barriers for shutting down the operation were implemented.

- Alarm in LabVIEW
- Overload sensor where an electrical signal cuts power
- Automatic power cut when drillstring approaches winch

The Gantt-diagram in Figure 25 was created to keep progress on schedule. Green indicates progress and red indicates task still to be completed as of March 25th. The names indicate persons who are responsible for aiding in the process. The overall responsibility for the project execution and follow up of each task lies with the author of this report.

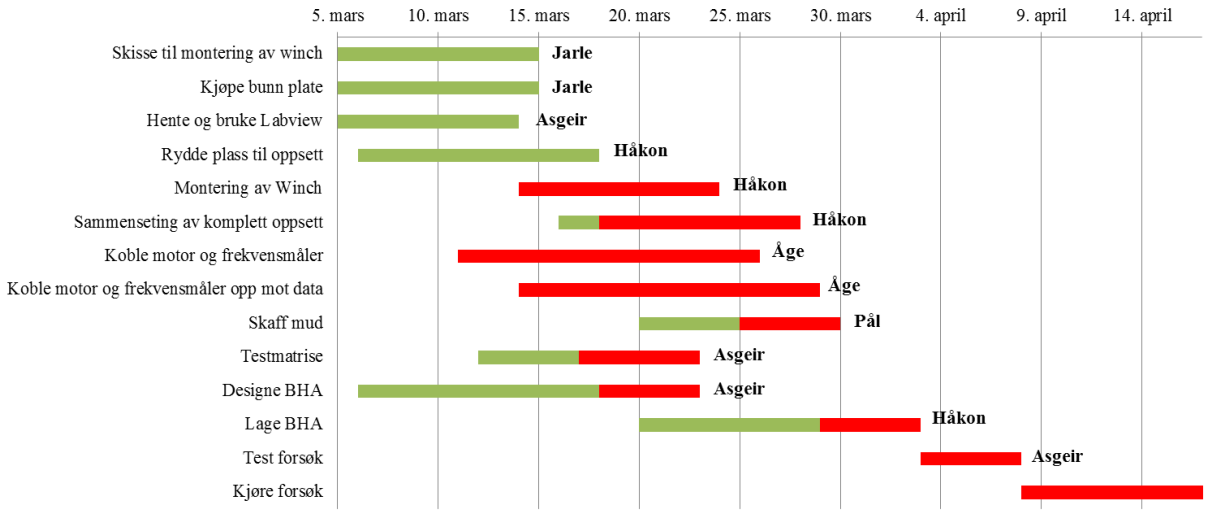

Figure 25: Plan and progress around the 25. March. Green indicates completed work while red denotes work that still needs to be completed.

All components in the laboratory set-up had to be custom crafted or specially ordered. As a result, several unforeseen delays caused the original schedule to be revised several times. Specifically, milling of components to the winch and construction of other parts in the workshop accounted for the longest postponements. In addition, the special equipment, such as the position meter, took a long time to arrive. The final problem occurred when initial testing began. The hook load readings had disturbances when the power of the winch was turned on. This was deduced to be a result of interference from the frequency convertor. A lengthy discussion of this problem is included in later sections.

Upon completion, the Gantt-diagram in Figure 26 illustrates the actual period of the build. There had been a change in lay-out in order to better keep track of time. As with the first figure the names are for who assisted with the tasks. The final responsibility lies with the author of the report.

ID	Activity/Task	Start	Finish	Duration	% Complete
1	Sketch for assembly of winch	05.03.2014	14.03.2014	1,6w	100%
2	Buy plate for winch	05.03.2014	14.03.2014	1,6w	100%
3	Collect and install Labview	05.03.2014	14.03.2014	1,6w	100%
4	Clear space in IPT-hall	10.03.2014	20.03.2014	1,8w	100%
5	Assembling first part of set-up	17.03.2014	25.04.2014	6w	100%
6	Connecting frequency counter and motor	17.03.2014	05.05.2014	7,2w	100%
7	Obtain cuttings	05.03.2014	28.03.2014	3,6w	100%
8	Design BHA 1	05.03.2014	21.03.2014	2,6w	100%
9	Make BHA 1	21.03.2014	04.04.2014	2,2w	100%
10	Inital Testing	28.04.2014	20.05.2014	3,4w	100%
11	Design BHA 2 & 3	26.05.2014	04.06.2014	1,6w	100%
12	Assemble Complete Hook Load set up	05.05.2014	23.05.2014	3w	100%
13	Complete Electrical Circut Set-Up	05.03.2014	21.05.2014	11,2w	100%
14	Make BHA 2 & 3	26.05.2014	05.06.2014	1,8w	100%
15	Design fluid System	28.05.2014	29.05.2014	,4w	100%
16	Construct Fluid system	30.05.2014	03.06.2014	,6w	100%
17	Initial test	03.06.2014	05.06.2014	,6w	100%
18	Complete testing	05.06.2014	13.06.2014	1,4w	30%

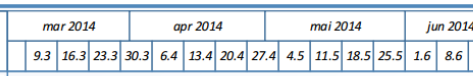

Figure 26: Gantt-diagram showing progress as of 08.06.2014

6.2 Design and building of hook load rig

The physical model went through several versions and rough drafts before completion. Figure 28 shows how the finished model was designed and organized. In the following, each main component of the apparatus is described and discussed.

A large steel beam was cut at 5 meters and attached to the floor with several bolts. This was done to keep the frame from buckling. Figure 27 illustrates the danger of buckling in a tripping situation in the laboratory.

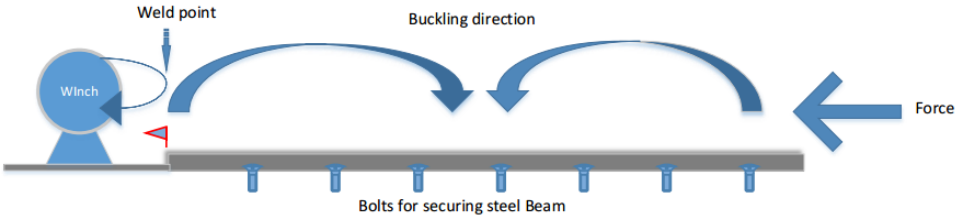

Figure 27: Potential buckling direction during pulling of drillstring

The winch was bolted onto a steel plate and welded to the steel beam. A holding section for the pipes was cut from a steel plate. The holding section for pipes was welded to the other end of the steel beam. This allows for a "screw–on, screw-off" system for pipes.

The current setup compromises two pipes connected at a joint. This maintains flexibility when testing. It is easier to test at different lengths and to attach BHA. The total length of the pipes are 5 meters, which means the limiting factor when pulling the drillstring is the steel beam.

A simple fluid circulation system is attached to the set-up. At the back end of the pipes, there is a water supply. In this setup the water functions as drilling mud. At the other end, an opening allows fluid to exit. Attached to the exit is a flowmeter for measuring the flow out of the pipe. The circulation resembles the mud system on a drilling installation. For future scenarios, another fluid could replace the water without too much difficulty. On the current set-up the water supply

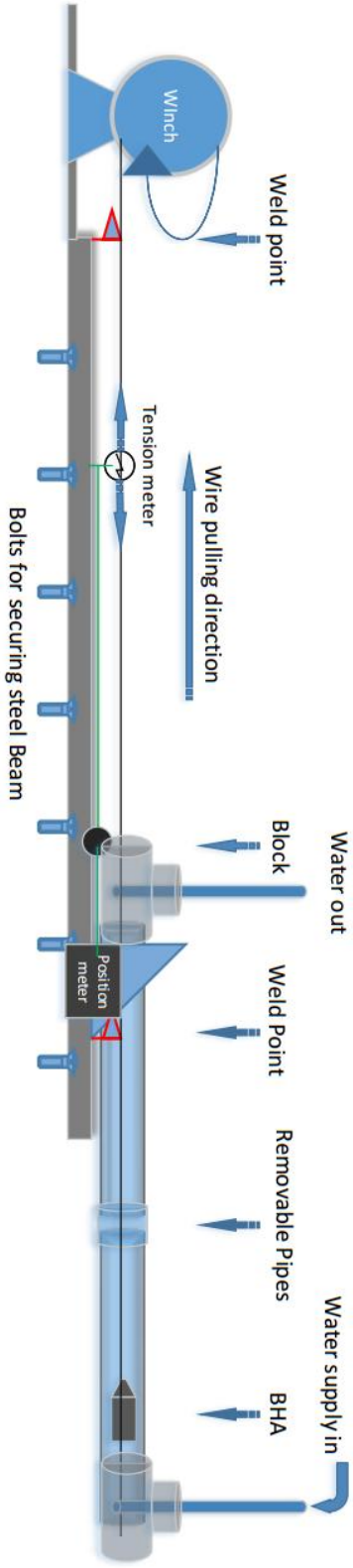

Figure 28: Rotated view of the complete setup of hook load rig

in can be detached and an air pressure hose can be connected instead, as shown in figure 29. This allows for removal of cuttings and water out from the pipes.

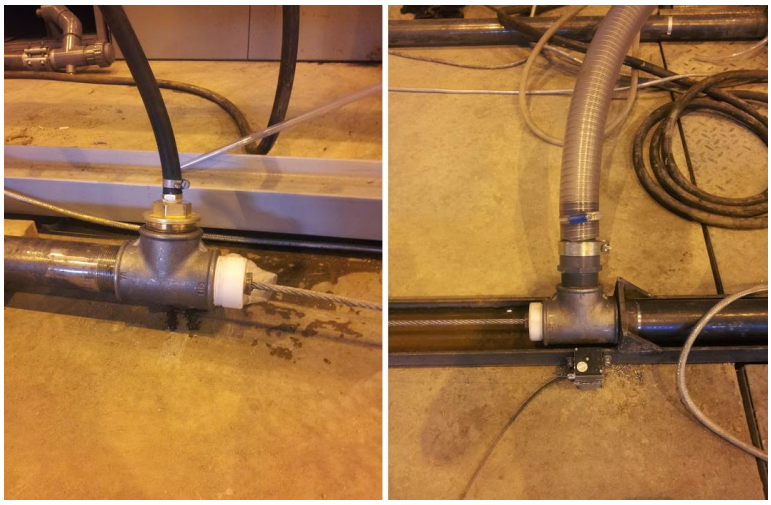

Figure 29: Water/mud circulation system at each end of the borehole

One of the goals of the experiments is to create a stuck pipe incident. This is when the drillstring and BHA become stuck in the borehole. When a stuck pipe incident occurs, the pulling force of the winch may be several hundred kN. In order to free the stuck drillstring after an experiment ta metal plate was bolted to the floor behind the hook load rig and a hook attached to the metal plate. Figure 30 illustrates how the freeing of stuck drillstring works. A jack connects to the metal plate and a tighten clamp. The tighten clamp grabs hold of the drillstring and the BHA is pulled free.

Figure 30: Jack and tighten clamp attached to drillstring to free stuck BHA

When pulling the drillstring an emergency stop function will cut the power to the winch if the string is pulled too far. The emergency stop function will automatically pull the power plug from the socket, stopping the rotation of the winch. This will prevent the winch from dragging the load cell into it. The positon meter has a max string length of 2 m. The emergency stop prevents severing of the wire and the string pulling out of its range.

6.2.1 Equipment

Several components were designed and custom made. This section presents a few of the most important componetns and solutions.

Winch:

Several components were milled in the workshop for the winch. The drum for the wire and engine brackets were the most important parts. Figure 31 shows the assembled winch with the wire attached to the drum.

Figure 31: Assembled winch

Load Cells/Tension Meters:

There are two load cells used for measuring the pulling force. Both give out 2 mV/V, are connected to a 12 V power supply and have a max force of 2000 kg and 200 kg respectively. From eq.23 this gives them an output of 24 mV at max load.

$$24\ mV = \frac{2\ mV}{V} * 12\ V \tag{23}$$

For recording hook load in range of a few kilograms the 24mV signal becomes an extremely low figure. When connected to the amplifier and multiplied by 1000, the new max output voltage becomes 24 V. This is a more manageable signal. A linear scaling, expressed in eq.XX, can then convert voltage (V) to kg (m). The minus seven is a factor for setting the starting point at zero.

$$m = 83{,}33\,V - 7 \tag{24}$$

However, it is worth noting that since the power supply is 12 V, half of the max tension force is available. When amplified 1000 times it is important not to exceed this limit as it cannot record the forces above 12 V, and the user loses control over the tension force.

$$24\,V = 24\,mV * 1000 \tag{25}$$

Figure 32 shows the load cells and below them is a plastic board. It provides isolation between the load cells and the steel construction, thereby preventing metal contact and reducing noise.

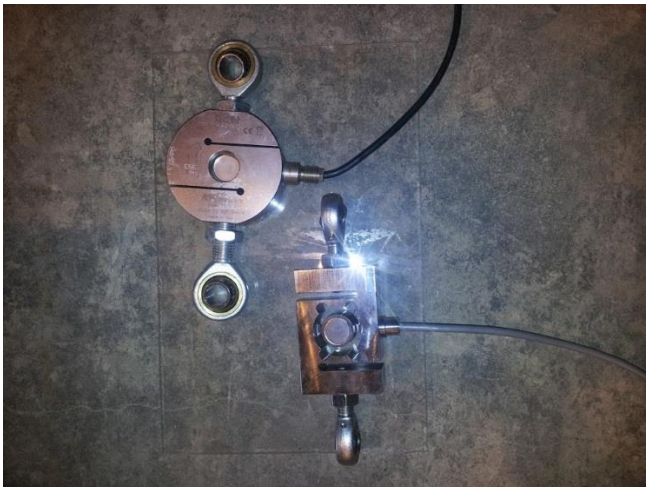

Figure 32: 2000 kg (upper left) and 200 kg (lower right) load cells/tension meters

BHA:

There are three BHAs currently made and tested in the lab. Each one was milled from steel and have a density of 7842 kg/m^3. Table 2 lists the specifics of the BHAs. The design of the first BHA was for testing and is heavier than the rest. This was in order to make sure the static friction force could be registered by the load cell. The diameter is 52 mm which provides a clearance of 2 mm from the pipe simulating the borehole.

The conical shape to the very right in figure 20 is the BHA 2. The third BHA has a stepped conical shape. It has a sharp angel until the diameter is 40 mm then the angel slacks off until the end diameter is 53 mm. It can be seen to the left in figure 33. The design of the last BHA was to ensure cuttings shoveling would occur, along with a stuck pipe situation.

Figure 33: BHAs milled in the workshop. From left to right: BHA 3, BHA 1, and BHA 2

Both BHA 2 and 3 were designed for cuttings accumulation and to check which effect, under the same conditions, the effect of BHA design would have on creating a stuck pipe incident. Each of the BHAs have a 9 mm hole through the center of them to allow for connecting to the drillpipe. The drillpipe in the experiments is a 10 m and 8 mm thick wire.

Table 2: Weight and dimensions of HKL equipment

Parameter	BHA 1	BHA 2	BHA 3	Wire(Drillpipe)	Pipes
Diameter at end	52mm	53mm	53	8mm	54mm
Length	20 cm	30	20	10 m	5 m
Weight	2,914 kg	1,2 kg	2 kg	2 kg	n/a
Inclination	60	30		n/a	90
Diameter at midpoint	52		40	8 mm	54mm

During testing with water, the set-up leaked from the entry and exit point of the drillstring. As a counteractive measure, two plastic ends were milled in the workshop with a 9 mm hole through.

A larger hole was then carved out at the end and filled with a rubber as a seal, before a screw was attached at the end. The inside of a seal and the finished product could be viewed in figure 34.

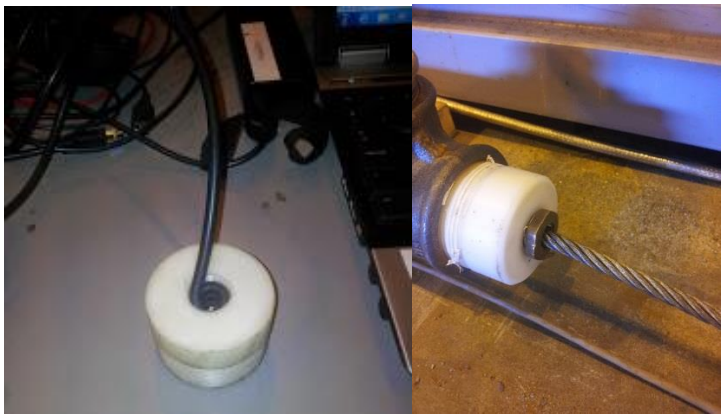

Figure 34: Creating water seal for the end of the pipes. Figure shows the insertion of the seal (left) and seal when connected to the end of the pipe (right). A screw was attached to the top to secure the seal.

Positon meter:

When measuring the position of the drillstring one criteria was that the rate of the measurements was the same as the hook load recording rate to have a corresponding value at all times. However, the maximum length of an available positon meter was 2 m. To solve this problem an arrangement including a block and an extra string were made. The string is attached to the drillstring, then threads through a sheave on the block and is attached to the steel beam. The positon meter string is also attached to the block. The result is that the total pulling length doubles and the total length/position meter range is now 4 m. Figure 35 illustrates the principle

.

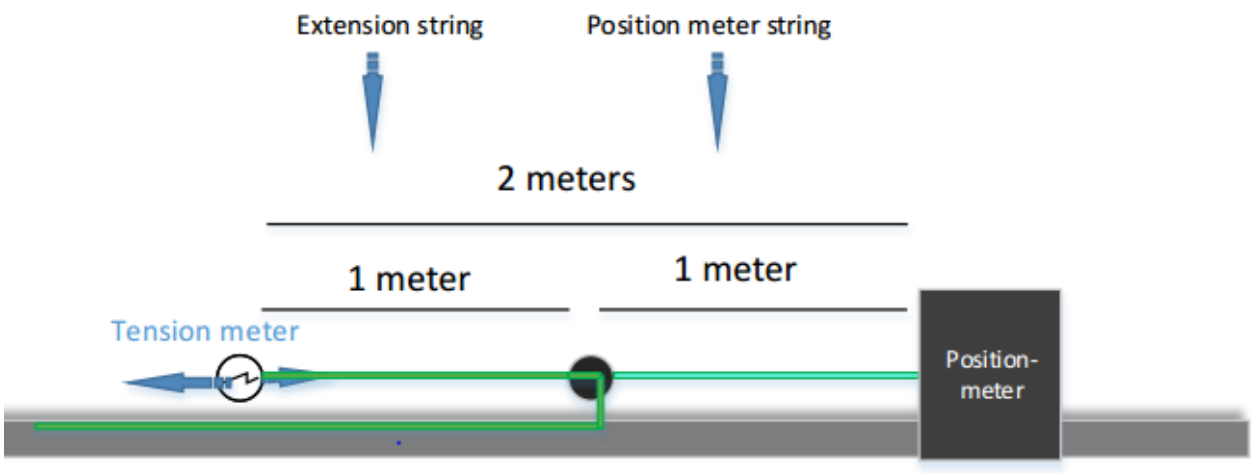

Figure 35: Principle of added pulling length to the position meter.

For example, when the drillstring travels two meters the position meter only had travels one. To make up for the increased pulling length the scale was adjusted by a factor of two.

Flow Meter:

To investigate how restrictions effect the flow (q) a flow meter was connected to the end exit point of the fluids. From the theory in chapter 4 it was established that when a stuck pipe due to cuttings accumulation occurs, the flow in and flow out should be constant. This causes the pressure to build up in the borehole (pipe) below the sticking point, and could eventually lead to a loss to formation (burst of pipe). However, as pressure builds up in the model, fluid leaks through the siege at the end of the pipe.

The flow meter has an output of 2-5 V where 2 V is no flow and 5 V is 50 l/min. The flow meter was scaled to:

$$q = 5\,V - 10 \tag{26}$$

6.2.2 Electronics

To make the lab equipment functional several converters, amplifiers and frequency counters were necessary. Figure 36 shows some of the most central components.

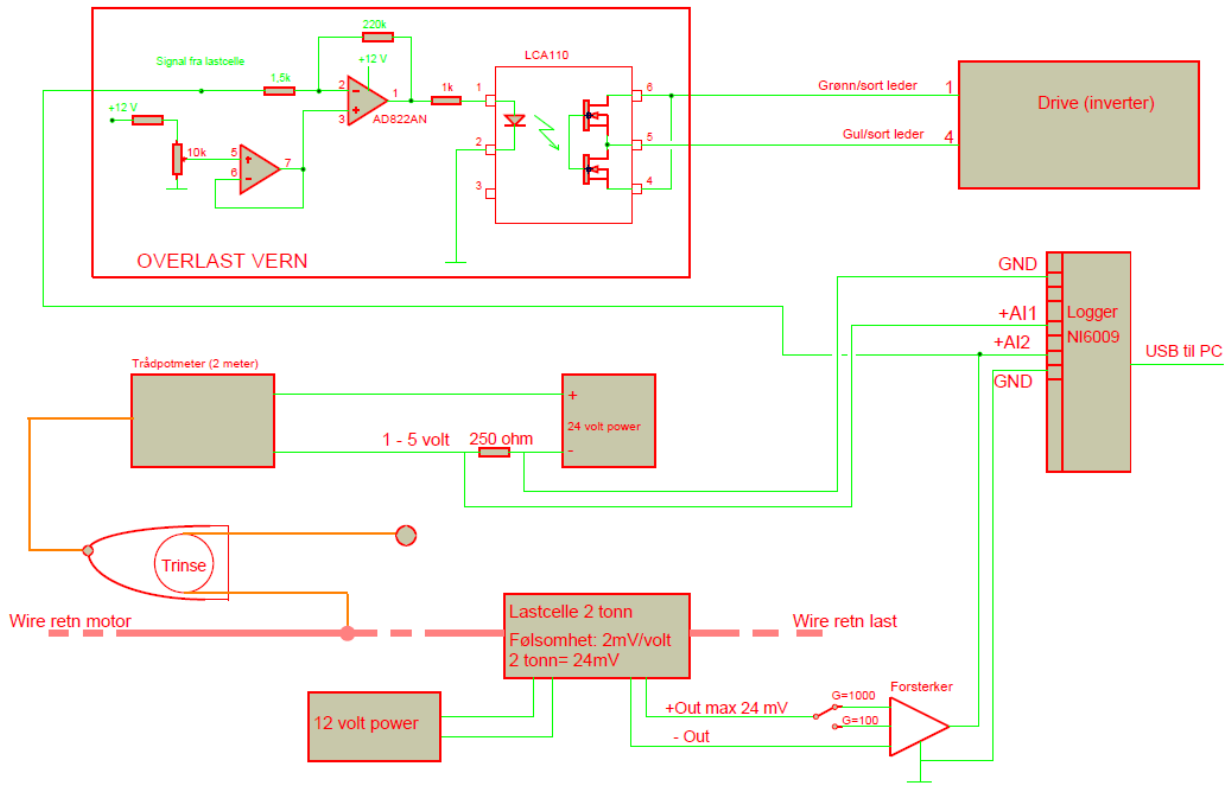

Figure 36: Electronic schematics for hook load rig.

An isolated wire runs from the power drive to the winch. The wire is isolated in order to reduce noise. The frequency converter has a power net isolator

A component to switch the pulling direction had to be connected to the winch in order make it rotate in both directions. This switch controls starting the tripping operations. The component could not be isolated and is a possible source of noise.

A power converter supplies the load cell with a 12 V power supply. Attached to the load cell is an amplifier with two settings. It can increase the signal by a factor of 100 or 1000. It can alter

between the settings by a switch. The signal then goes to the logging device along with the position meter signal.

As a safety feature, the load cell connects to an overload sensor that then connects to the power drive. The high forces during stuck pipe testing can potentially cause harm to personnel and equipment. To prevent the wire from exceeding its tension limit and/or bending and damaging the pipes, a max limit can be set on the pulling force. A voltmeter reads the voltage from the load cell and cuts the power electrically when it exceeds a specific value given before the test commenced.

The schematic was made when frequency problems arose during testing. It was used as a problem-solving tool in discussions with experts from the industry. Contact was established with Aker MH and Transocean in order discuss possible causes of the noise and interference problems. It was recognized that noise and disturbances in the general power grid originating from feedback from frequency converters and drives are well known problems in the industry. Steps taken to reduce noise are given in chapter 8.

6.3 Running the Experiments

This section will give an understanding of the control systems involved, operating instructions for the apparatus and the procedures for running an experiment.

6.3.1 Lab View

LabVIEW was found to be the most appropriate software to control and record the results of the experiments. The advantage lies in the possibility of using built in functions, which are called VI's (virtual instruments), along with the easy access of instrumentation data, and built-in functions for data acquisition. LabVIEW consists of two user interfaces; the Block Diagram and the Front Panel. On the Block Diagram all the programming is done and different VI's are attached to each other. The Front Panel then displays the data from the programming.

LabVIEW is a visual programming language. This implies that the user can access VI's such as graphs, charts and other functions. The VI's can then manipulated through a functions and programming palette which gives the user further options in developing the program.

The LabVIEW set-up for controlling the hook load experiments consisted of several points.

- NI USB-6009 is used to collect the analog data from the load cell, position meter and flow meter
- Individual charts displaying hook load, block position and mud flow out
- A graph showing the block position and hook load together
- A limit function that alerts the user when the hook load or block position overrides a predefined value.
- Calculation of theoretical hook load using equations and theory from previous section in this report
- A write to measurement file function that enables the user to export the data to Microsoft excel.

A NI USB-6009 device, heron referred to as DAQ-assistant acquired the data. It converts the voltages from an analog signals to voltage in LabVIEW. The voltage can be read directly on the charts and graphs in LabVIEW.

The obtained voltages can be scaled and manipulated to output in the desired format. For this set-up, the appropriate values were set as kilograms for the hook load and meters for the block position. A direct conversion from volts to a corresponding value was programmed in LabVIEW. This allows for the correct hook load weight and block position to be recorded directly on the front panel.

Figure 37 shows the programming and wiring done in LabVIEW. The structure of the code is split in two. The top half is where the DAQ-assistant collects the data from the experiment.

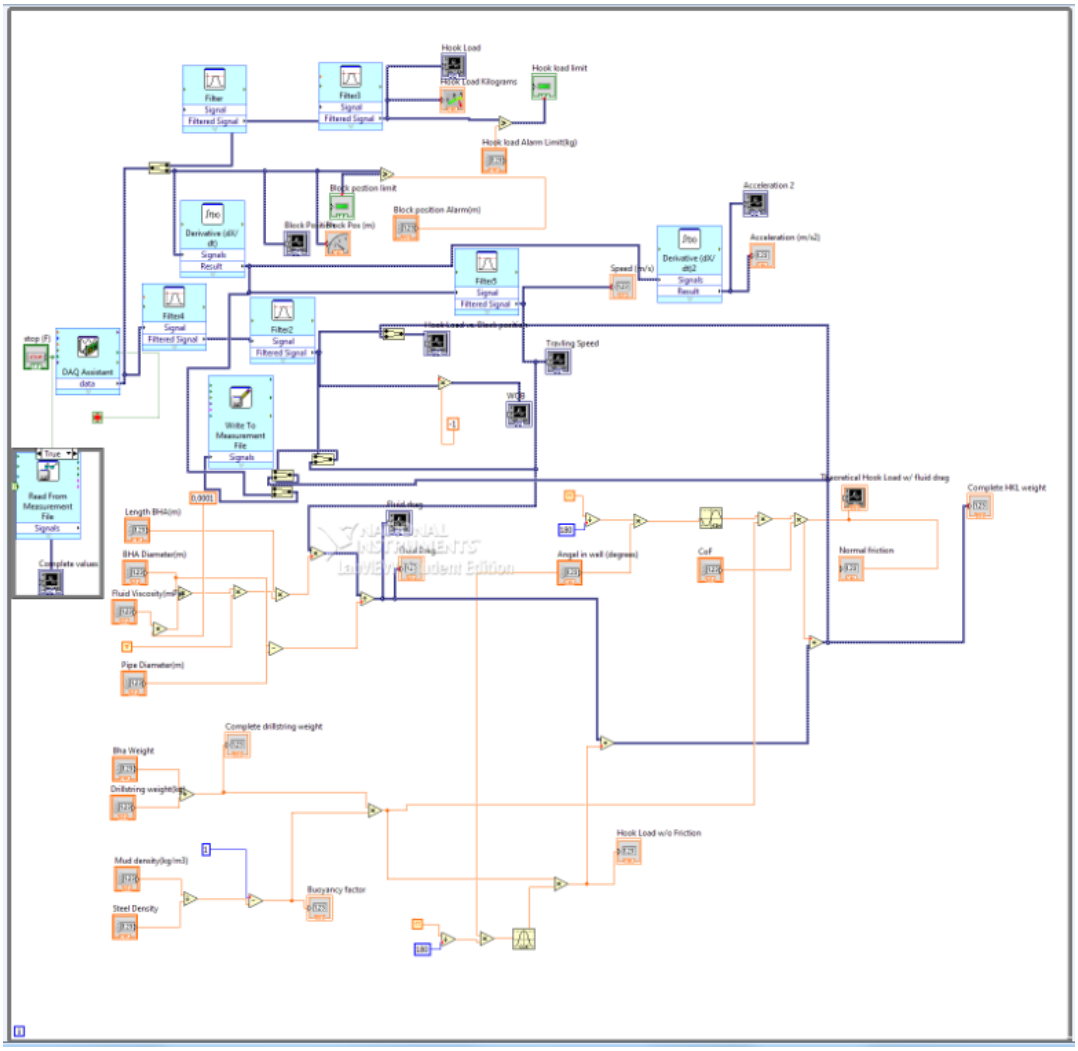

Figure 37: Block diagram with coding for running HKL test.

The DAQ can collect the data up to a specified 1000 Hz and the graphs and charts show the data continuously at this rate and only short glimpses of the data are seen. To counteract this the entire code is inside a while-loop. The loop makes the iterations inside repeat until the simulation ends by pressing the stop button on the front panel. This enables the program to show the data as a continuous curve. On the data from the hook load cell there are two filters. A low-pass filter followed by a smoothing filter contribute to generating a more even curve. Adding the filters was necessary because of large interference and noise on the hook load signal, mainly from the winch frequency converter. Presentation and discussion on these are in the in the results and evaluation section respectively. All gauges, alarms and charts seen on the front panel are placed here.

The bottom of figure 31 shows the calculations for the theoretical hook load. The calculations and equations originates from the theory presented in chapter 3 of this report.

During experiments, the front panel displays the data collected from the DAQ-assistant and consists of these main features:

1. A chart that runs continuously displays the curves
2. A graph that generates the entire experiment after it is stopped
3. Indicators for to easily keep track of block position and hook load
4. Alarms that turn red if the vales exceed a specified value. Two number indicators are placed next to the alarms for specifying limit values.
5. Charts where each of the tripping parameters and calculations are presented separately
6. Displays the calculations from the theoretical hook load. The calculated parameters are:
    -drillstring weight
    -buoyancy factor
    -fluid drag
    -drillstring weight when submerged in a fluid
    -the friction force
    -velocity
    -fluid flow out of pipes
7. Numeric controls where the parameters for the experiment are entered
8. A WOB graph that is programed to show when the hook load becomes negative. This is because the hook load and WOB or inverse curves in ideal conditions.

The entire front panel that was created for controlling the experiments is shown in figure 38. The two large screens at the top left give most of the parameters in the same window. The one to the left is updates in real time as an experiment is conducted. The one to the right automatically generates an overview of the entire period, when the stop bottom on the screen is pushed.

The bottom row is a graph for each one of the parameters that generates in real-time. To the very right is an indicator panel for important values during the testing. These also update in real-time. The middle right is where the specifics for the experiment are entered. The calculations in the program uses these numeric values. The parameters that need to be filled out are:

- BHA diameter (m^2)
- BHA length (m)
- BHA weight (kg)
- Drillpipe weight (kg)
- Viscosity (mPA)
- Mud density ($kg/m^{3)}$
- BHA density (steel) (kg/m^3)
- CoF

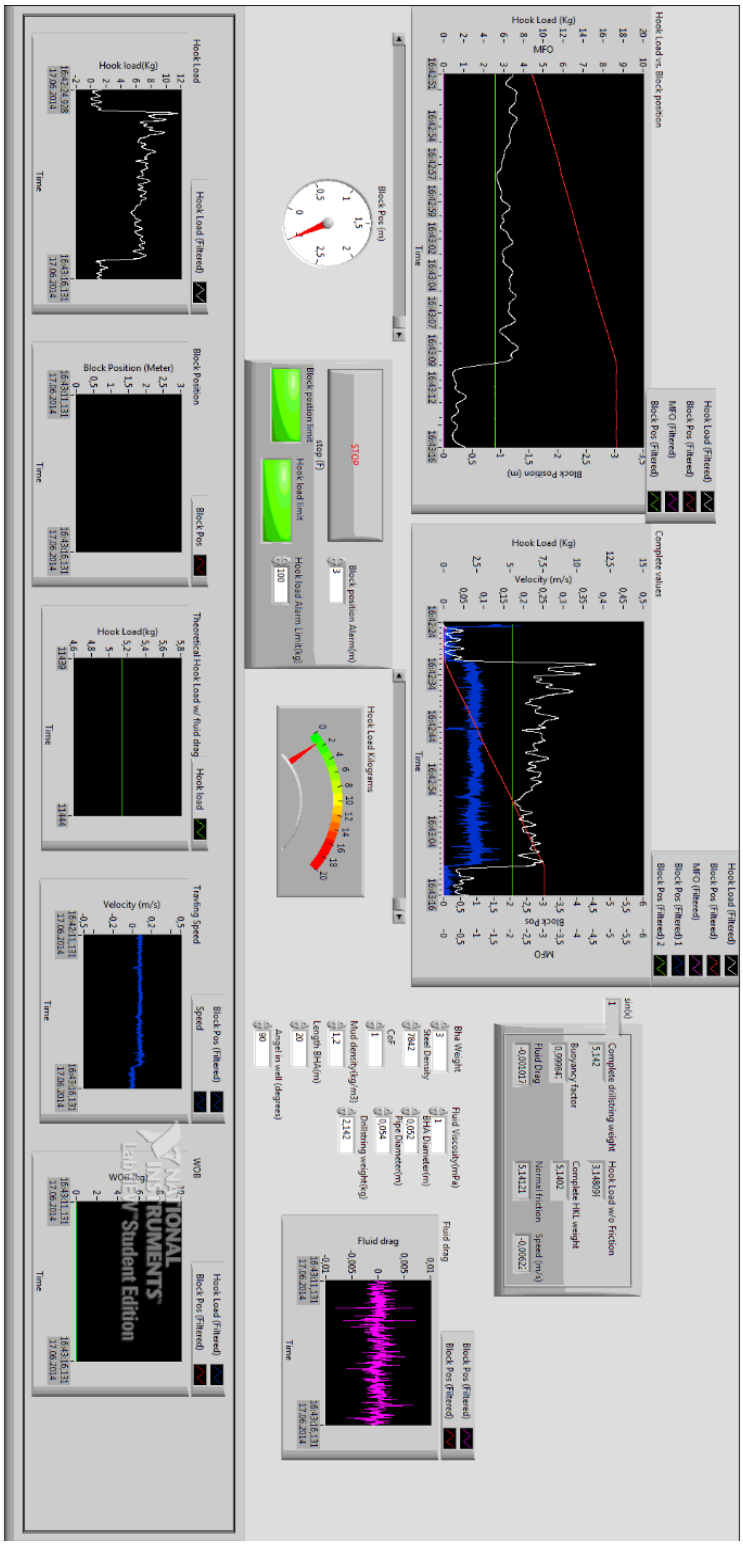

Figure 38: Rotated view of the front panel for monitoring of hook load experiments.

6.3.2 Procedures

Several procedures were established. For easier visualization a flowchart (figure 39) shows the procedure to start a new hook load experiment.

- Set the safety parameters: The first step is to set the max voltage on the overload sensor, then set the max hook load weight and max tripping length in LabVIEW. Another important factor to consider is to keep all cables and wires physically separated in order to reduce noise and interference on the signals.
- Prepare the drillstring: Insert first, a plastic seal slides on to the drillstring. Once a BHA is selected, the wire is slid through the hole through the BHA. Then secure it to the wire by fasting the bolts on the wire-stoppers. There are two on each side to keep the BHA from sliding. The pipes, which function as the borehole during the simulations, are screwed on to the steel beam. This is done by sliding the pipe through the hole in the steel plate and securing it to the T-connection on the other side of the steel plate. The water supply is also attached to each end of the T-connection. Finally, the last plastic seal slides onto the wire and screws onto the pipes. Figure 18 in section 6.2 shows each end of the set-up. If a stuck pipe experiment is conducted the pipes are disconnected at the middle and filled with cuttings, before reattaching them. Position the drillstring so that the block position shows zero.
- Pulling operation: Select a pulling velocity for the experiments and start the program in LabVIEW. The front panel on the LabVIEW now continually displays the data from the experiment. Start the experiment by switching the winch control to POOH.

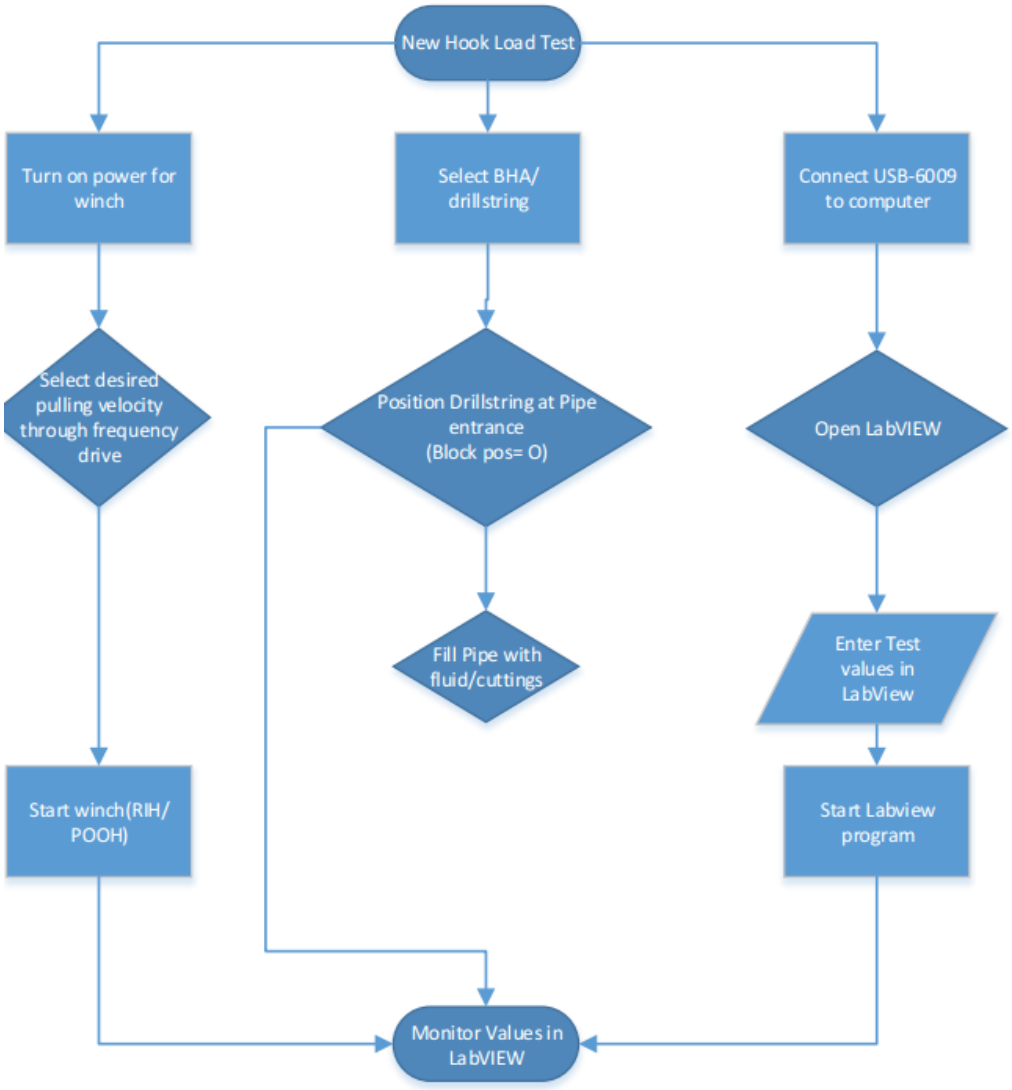

Figure 39: Flowchart for running Hook Load experiment.

- Pulling out: When an experiment is concluded the winch is switched to RIH and the BHA can be pulled out of the back of the pipe.
- Prepare new run: A new BHA can be attached and a new experiment can quickly be commenced. If the experiment was with fluid in the pipe, attach the air supply to the back of the pipe and blow out the water before pulling out the BHA.

- Freeing stuck pipe: It is necessary to give procedures for freeing stuck pipe also as it is not intuitive and an important part of the design.
    1. RIH with drillstring to release tension in drillstring
    2. Attach tighten clamp
    3. Pull on jack to free BHA
    4. Once free connect air
    5. Blow the cuttings to clear restriction
    6. Continue POOH

6.4 Test matrix

To provide an overview of the tests conducted on the hook load rig a test matrix is included. The testing was conducted in three parts. The first testes performed to check if there were any problems with the design of measurements. The tests performed at three different data collecting rates to determine if rate would have any effects on curves. In addition, they were conducted at different velocities to see the effects of different frequencies. Secondly, initial testing to determine if the rig was capable of recreating hook load signals resembling the normal signature established in chapter 4.

Table 3 lists the initial testing trails. All the tests in table 3 were done with BHA 1 from table 1.

Table 3: Test matrix from initial trails

Condition	Velocity	Measurments/second
DRY	12,5 Hz	3
		10
		100
		1000
DRY	5 Hz	3
		10
		100
		1000
DRY	25 Hz	3
		10
		100
		1000

Table 4 shows the final part of the testing. The goal of these tests were to simulate the hook load signatures from section 4. If a signature resembling the hook load from theory and RTDD data could be simulated, the curves could be further evaluated. The tests with cuttings indicate restriction testing.

To determine the effect of cuttings size on hook load restriction signals, two types of cuttings size were used. These can be seen table 4. The cuttings are volcanoclastics collected from a land drilling operation in Slovakia. The drilling operation is classified and therefore it was not possible to provide further information about the cuttings.

During drilling operations, each new drillstring is referred to as a run. In the following chapter each test will also be called a run. All measurements recorded at 100 measurements per second. The velocity of 12,5 Hz is approximately 0,08 m/s while 5 Hz is approximately 0,03 m/s.

Table 4: Final test matrix for experiments

Condition	Situation	Velocity	Cuttings size	BHA 1	BHA 2	BHA 3
DRY	No cuttings	12.5 Hz	n/a	x	x	x
		5 Hz	n/a	x		
	Cuttings	12.5 Hz	0,1-2 mm	x	x	x
			1-7 mm			x
		5 Hz	0,1-2 mm	x		
FLOW	No cuttings	12.5 Hz	n/a	x		x
		5 Hz	n/a			
	Cuttings	12.5 Hz	0,1-2 mm	x		x
			1-7 mm	x		x
		5 Hz	0,1-2 mm			x

7 Results of the Hook load model experiments

This section presents the results from the testing and procedures presented in the previous section. While several more were conducted in the qualifying of the hook load rig, the test matrixes (Table 3 & Table 4 above) illustrate some of the most important tests. The parameters in Figure 40 represents different parameter signal color in the LabVIEW output. A legend will also follow each of the following figures in the section.

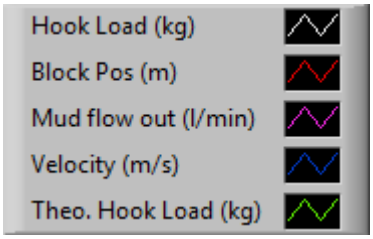

Figure 40: Legend for graphs.

The measurements in this section will be recorded at 100 Hz (100 measurements per second) unless otherwise stated. It was concluded that this rate was more than sufficient for its purpose of displaying hook load signatures and revealing trends. This section will also presented how this conclusion was reached.

Not all tests in table 3 (above) will be presented explicitly, only relevant information like typical results, trends, and anomalies, if any, will be presented.

7.1 Trial runs: Interference Issue

The first runs were conducted to check the how the measurements behaved and if the response would be as expected. Figure 41 shows the initial measurements. It shows heavy fluctuations. Disturbances were recorded on the hook load signal while the block position measurements remained unaffected. The largest variations exceeded several hundred kilograms where the expected hook load was around 5 kg. This is referred to as noise. It is a common problem when dealing with electronic equipment and in particular equipment involving frequency drives and converters for regulation of output. In the upper graph in figure 41, there are no filters or other steps taken to reduce the noise. In the middle, the frequency drive has been isolated and the load cell has been placed on a plastic plate to remove metal contact. Additionally, all the equipment has been grounded. The bottom graph shows results after filters have been introduced in LabVIEW.

Before further testing could commence, reducing the noise was necessary. Through a process of deduction, the origin of the problems was located. From the top curve in figure 41, it can be seen that the fluctuations are occurring at a regular rate. The problem was traced as interference from other electrical equipment, particularly the winch's frequency drive. When shutting down the frequency drive for the winch the hook load signal stopped fluctuating and receded to expected value.

Several physical steps were taken to reduce the problem, such as grounding all electrical equipment. In LabVIEW two filters were used to remove noise as. The first filter is a low-pass filter for frequency and the second is a smoothing filter. Additionally, discussions were held with industry experts on how to reduce the problem. The details on actions taken and solutions to the problem are placed under the discussion in chapter 8**.** Noise and interference is a common problem in the industry as well. A brief discussion on how the interference problem is solved on offshore platforms is also included in chapter 8.

The figures have been collected at zero tension in order to reduce variables when illustrating the noise.

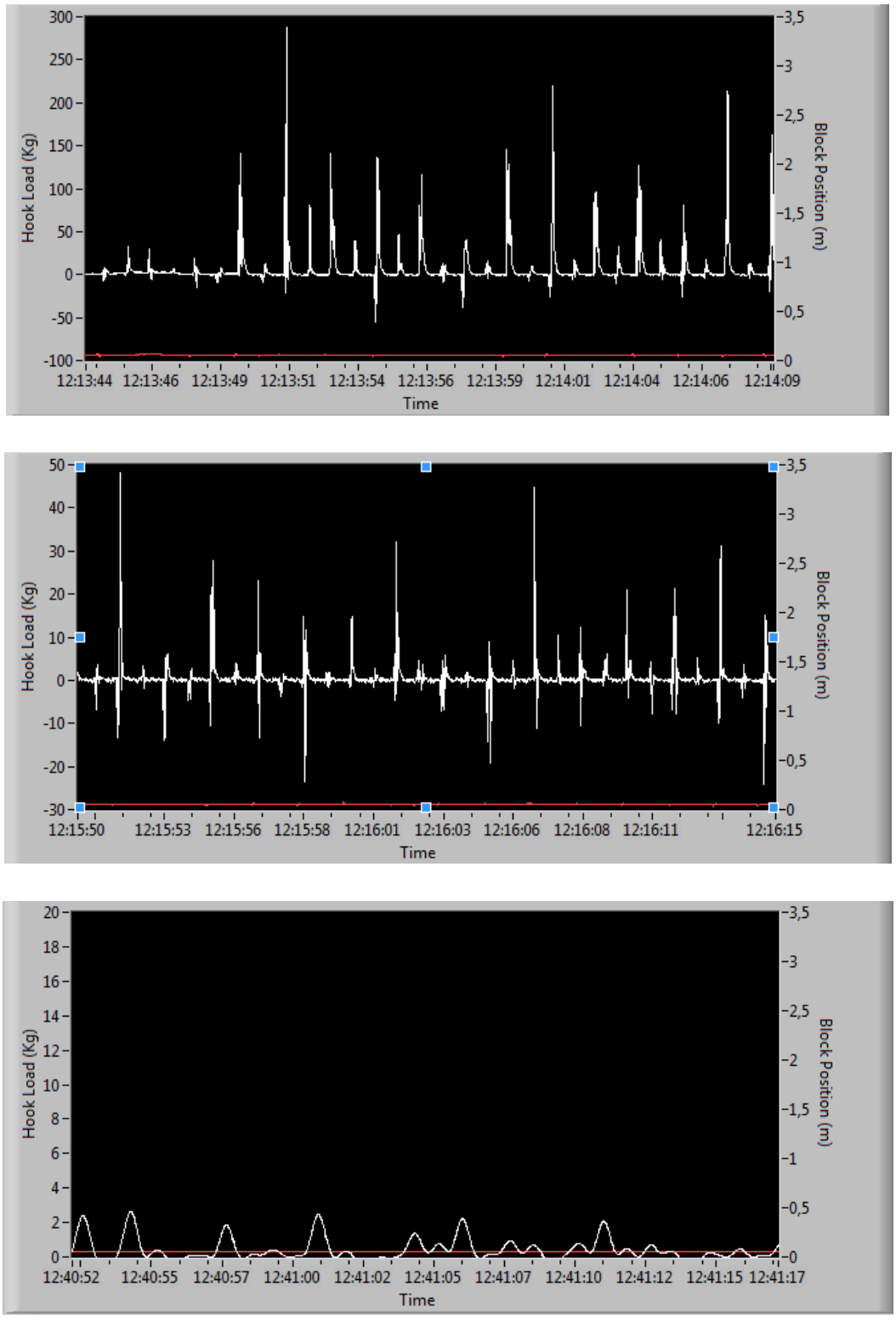

Figure 41: Different levels of interference. The top figure shows no steps taken tm\o minimize noise. The middle shows after isolation of load cell from steel beam, grounding and isolation frequency drive. The bottom is after filters are added in LabVIEW. Notice in particular the scale of the hook load weight.

7.2 Tests at normal hook load

Figure 42 shows a typical curve when tripping with no restrictions. There is high peak at the start followed by a slight reduction before the hook load settles towards the end. The old laboratory set-up had not been able to simulate the drillstring overcoming the initial friction (Glomstad, 2012). Both are partly mimicking filed operations: First peak corresponds to initial acceleration of the drillstring, before the kinetic friction takes over. This is a typical curve when tripping with no restrictions. The sharp drop is to indicate that the stand has been tripped out of hole. When the stand is pulled out, the drillstring is hung off on the slips on the drillfloor, causing the hook load to drop before picking-up the drillstring again. In the same way, the tension on the hook load rig releases by switching to RIH on the winch control. The figure is almost an exact copy of the norm Cordoso Jr, et.al (1995) established (see figure 12 above).

The test in figure 42 was conducted with no fluid in the pipe, no cuttings and BHA 1. Since BHA1 was used, the clearance between the pipe and BHA is 2 mm. The hook load signature for a run without restrictions was recognizable for every run, regardless of BHA.

An interesting observation is that the hook loads correlate to the velocity during tripping. The figure shows two dips in velocity accompanied by dips in the hook load curve. There is a slight delay of about 0,5 seconds before the dip in the hook load curve occurs. This is because of inertia. The phenomenon is highlighted on the bottom of figure 42.

Several runs were performed while testing for normal hook load. Each time the initial peak was observable, followed by a quick approach to expected hook load. The fluctuations experienced are in the ± 1 kg range and a result of remaining noise on the hook load signal. Running with fluids seemed to have little to no effect on the hook load curve. This is most likely a result of the horizontal inclination of the set-up, where the friction factor (CoF) is the overwhelming contributor to the recorded hook load. The hook load is slightly above the theoretical hook load, 5,1 kg, because the seals which were put in place to contain fluids in the pipe. The seals squeeze on the drillpipe causing extra friction.

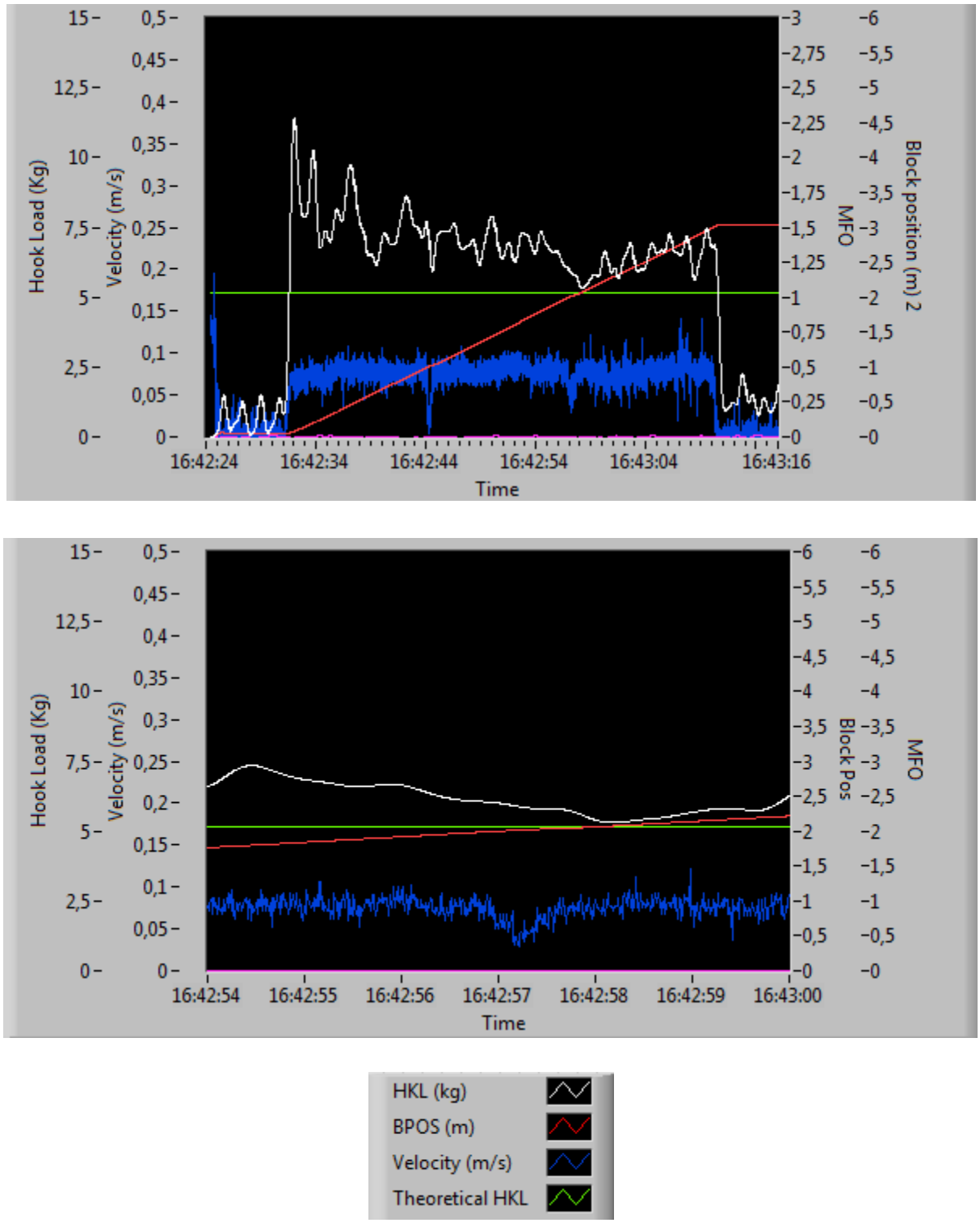

Figure 42: Hook Load variation during slow, steady POOH speed. The upper graph shows the entire run. It is a near identical match of the normal hook load curve from figure 12 presented in chapter 4. The bottom image highlights the velocity drop at 16.42.57 followed by hook load drop at 16.42.58.

7.3 Tests for evaluation of the data acquisition system

Several tests were performed to see the difference in rate of data acquisition. In the RTDD from field operations, the normal acquisition rate is one measurement per 2-4 seconds (0.3 Hz). An interesting comparison is to see how acquisition rates effect the hook load curves in the lab. Figure 43 shows two different rates. The upper figure represents a rate of 3 Hz while, the bottom figure represents 100 Hz. The two runs were conducted under the exact same conditions. BHA 1 was used in dry conditions. Table 2 in the previous chapter gives an overview of the runs performed.

The difference between the two hook load signatures is quite drastic. The run with 100 Hz provides much better detail as expected. When comparing the curves, the lack of signature when running with 3 Hz is evident. It lacks the initial peak and is constantly above the theoretical hook load. Towards the end, there is a spike. However, this is most likely a result of noise. A deeper discussion on the large difference is included in the evaluation in chapter 8.

The 100 Hz curve shows the initial peak and falls back to the expected hook load. In addition, it provides a much better curve for analyzing trends. The conclusion was reached that 100 Hz was sufficient. It provides clear detail while not being oversensitive to interference. Runs were also performed with 1000 Hz. However, the data proved more sensitive to noise for higher acquisition rates. At 1000 Hz, it was difficult to establish a trend.

The reason the 3 Hz hook load is above expected value is most likely because of the filters for noise reduction. One of the filters uses the previous values to average and smoothen the curve. The low acquisition rate means that values are sensitive to old values being averaged out. However, without the filter, noise was too large to exclude the use of filters. If additional isolation of noise and frequency drive disturbances is found, a lower sampling rate (i.e. lower frequency) may still be adequate. The experiment demonstrates the sensitivity of the processing of data and the necessity of understanding the effects of the error source. Noise due to frequency drive feedback represents an error in models and more importantly in real life applications. The details that can be observed at 100 measurements per second give contra 3 Hz, provides a curve for recognizing trends and signatures.

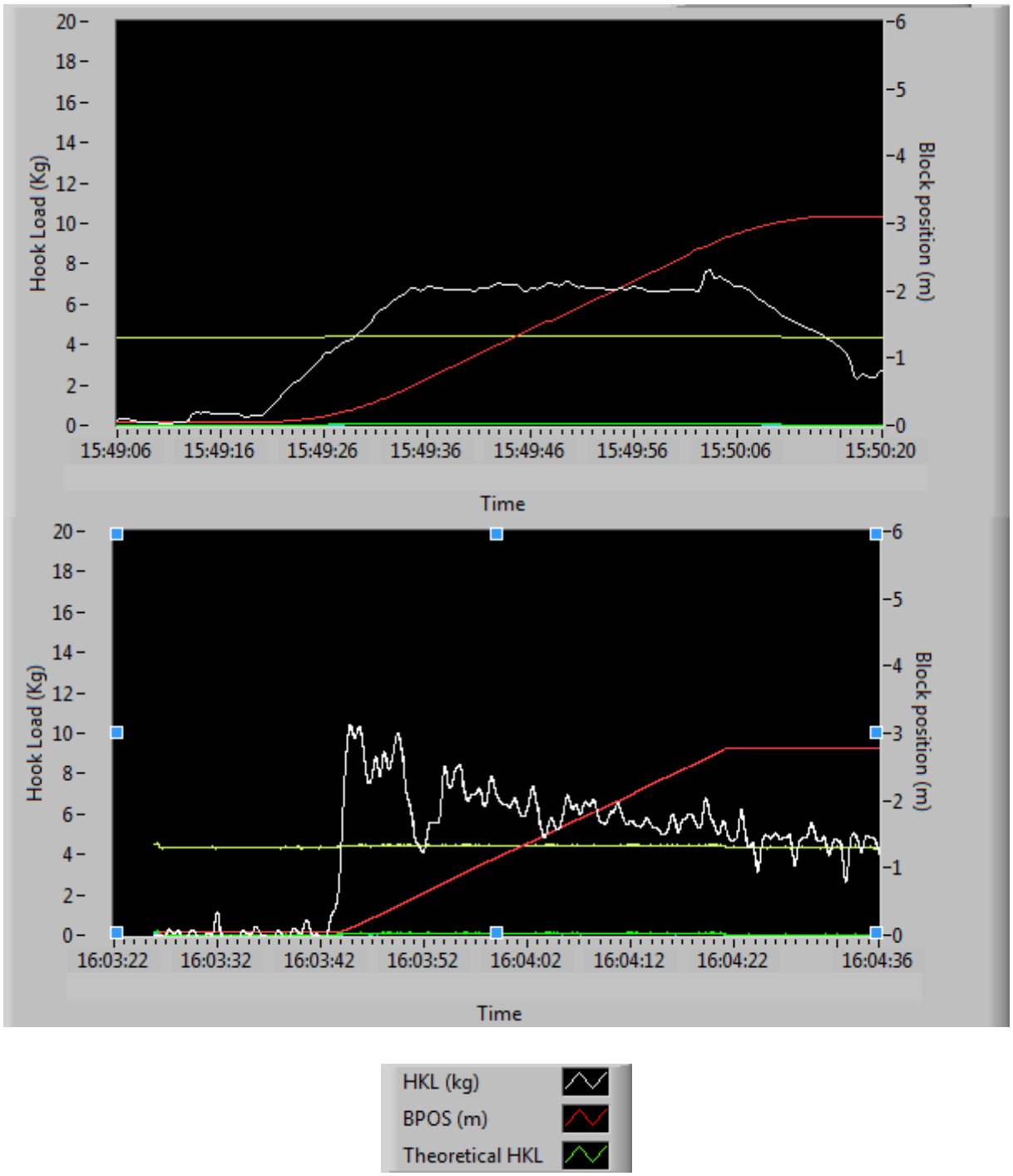

Figure 43: Hook load tests with two different data acquisition rates. 3 Hz (top) vs. 100 Hz (bottom) performed under the same conditions. Notice the lack of detail in the 3 Hz hook load curve. See chapter 8 for discussion on the difference between the curves.

7.4 Testing with restrictions

When testing with restrictions two types of cutting sizes were used as shown in table 4. The cuttings diameter were 0,1-2 mm and 1-7 mm. The pipe was disconnected at the mid-joint and the cuttings evenly distributed over the last 2,10 m in the pipes. Tests were conducted with flow and without flow.

Small cuttings-Dry pipe

When running with the small diameter cuttings in dry pipe there were no serious overpull events. The BHA did one of two things in these conditions as shown in figure 44:

- Shoveling the cuttings, but the restriction was too minor for the BHA to take heavy weight. The maximum overpull was 27 kg when the expected hook load was 5 kg. After the spike of 27 kg, the hook load stayed above expected value but only by a few kilos. The BPOS was unaffected by the restrictions. If a spring was introduced to the drillstring to resemble the spring effect inherent in a long drillstring, the block positon might have reacted differently. From comparison with typical signature profiles, the restriction signal resembled a ledge or key seat more than a cuttings accumulation signature.
- The BHA registered some resistance, but simply moved over or crushed the cuttings. When viewing the cuttings after the run, the grains were finer indicating that they had been deformed in the pipes. The crushing deformation of cuttings is based purely on observation when opening the pipes. This is a rough manual and has not been proven. In these cases the string took varying weight. It was difficult to conclude at what weight the cuttings became deformed and when the BHA simply moved around the restriction.

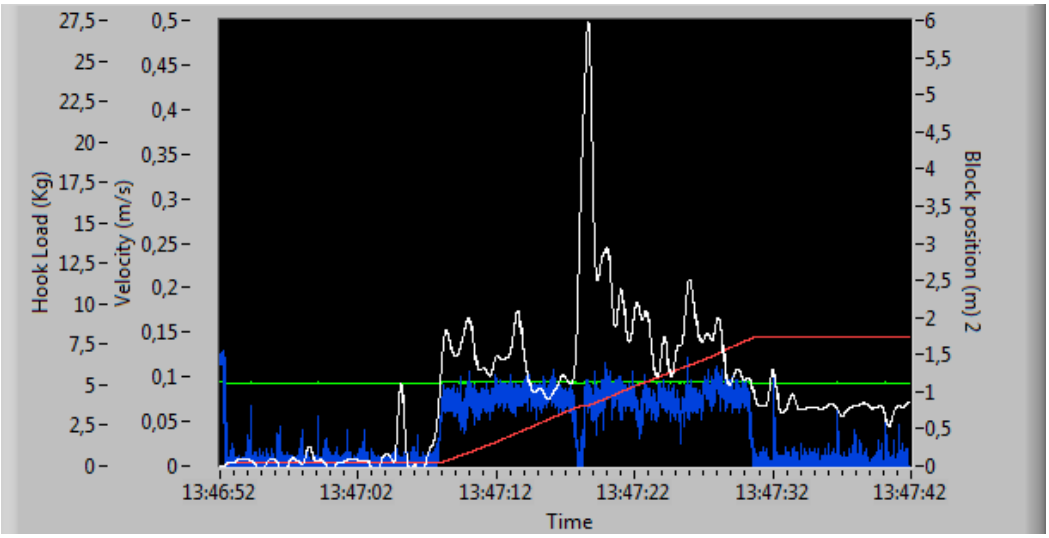

Figure 44: BHA moving over a restriction.

Small cuttings-Flow in pipe

The runs with small grains (0,1-2 mm) and flow in the annulus gave the exact same curve as the normal hook load. The flow carried the small grains away leaving no restriction for the BHA to encounter. Attempts were made to reduce the flow. These attempts proved futile, as the flow meter was not able to record any data at these low velocities. While not giving any new curve to analyze, this was taken as confirmation that the flow system works as it should. In the field, the desired effect is for the flow to carry away the cuttings.

Large cuttings-Dry

The tests with dry pipe and large cuttings (1-7 mm) gave heavy overpull. The largest one recorded was 600 kg. The overpull could potentially have been even larger, but the safety mechanism electronically cut the power as the set voltage for the run was exceeded. The tests with dry pipe and large cuttings constantly gave test with heavy overpull. However, once the restriction was observed the hook load immediately rocketed, giving no warning. These tests therefore provided little value, as they could give no indication of an approaching problem.

Large Cuttings-Flow in pipe

The final tests were conducted with flow and large cuttings.

Flows were varied and monitored through a flow meter. In figure 45, the flow was set at 20 l/min.

From eq.27 we see that the velocity of the flow in the pipe is:

$$0{,}12\ m/s \approx \frac{20\ \frac{l}{min}/1000/60}{(0{,}054^2\ m^2 - 0{,}008^2\ m^2)} \tag{27}$$

During these runs hook load signatures closely resembling stuck pipe situations were recorded. A steady build-up of hook load weight due to cutting accumulation can clearly be spotted in figure 45. This closely resembles Bjerke's (2013) symptom recognition for moving restrictions. Followed by the accumulation signature is a large overpull.

After the severe overpull had taken place, the weight dropped. The reason is that the safety voltage set was exceeded and shut down the power for the winch, releasing the tension in the drillstring. In a situation like this, a driller would in similar manner have stopped POOH and then have attempted to lower the drillstring. This would have also released the tension in the deadline and given a drop in the hook load. Had the voltage been set higher the outcome would likely have been a higher overpull, but with the same result. After the run, the BHA had to be freed using the jack-design at the back of the pipe

This case also brings a new parameter into the cuttings accumulation recognition. The flow in was kept constant throughout the run. Form the bottom of figure 45 the flow out experiences a reduction after the pipe is stuck. The reduction is due to the BHA and cuttings restricting the flow through the pipe. This causes a build up of pressure behind the restriction. This causes partial loss of flow through the seal at the end of the pipe. This could be compared to when circulation fluid is lost in the well to the formation due to pressure build below a restriction. The constant flow and buildup of pressure in the borehole is similar to the pack off case presented in chapter 4.

This case is a very accurate simulation of stuck pipe due to cuttings accumulation. For developing mathematical models, it could prove more useful than RTDD data, as it is a textbook example and includes less uncertainty than field data can provide, along with a higher data acquisition rate.

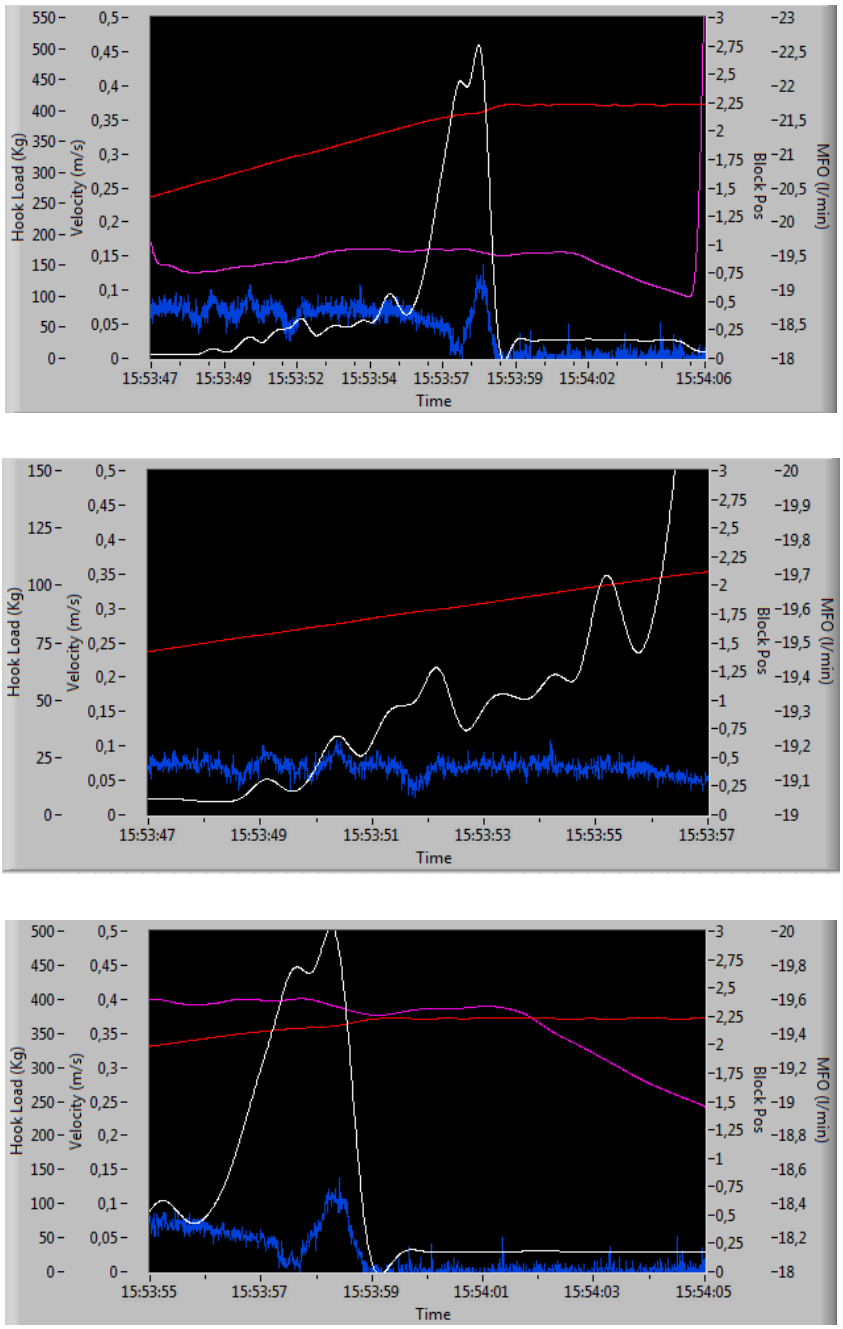

Figure 45: A stuck pipe simulation from cutting accumulation (top). A steady build-up of cuttings (middle) causes the hook load to increase until it becomes stuck with an overpull of 500 kg. The flow out decreases because the BHA and cuttings restrict the flow (bottom).

8 Evaluation and Discussion

The set goals and tasks for the thesis have been building testing and evaluating the hook load rig. This section is an evaluation of the results and the laboratory model. The discussion will be based on strengths and weaknesses of the new, developed hook load rig. Special focus is on the frequency issues and problems revolving around establishing a steady flow through the pipes. A suggestion for further work is also included. A brief discussion will be presented before the suggestions will be given in a bullet points format in order to increase the overview for students further developing the laboratory model.

8.1 Evaluation of Hook load rig

The built model comes across as a sturdy and robust design. It is capable of pulling safely very heavy loads. The maximum load during the course of these experiments was in excess of 600 kg. The model is capable of pulling much heavier loads. However, the safety discussion plays a part in the decision to restrict the pull capacity. The wire is designed for pulling 2 tons, as is also the tension meter. If anything were to go wrong at these forces, it could prove very harmful to equipment and to persons running the test. The worst-case scenario would be if the wire snapped creating a lashing movement. This is why alarms and safety functions have been incorporated in the set-up. It is therefore crucial that these are used and set properly, in order for the user to make a conscious decision on the maximum loads for a test.

In its current state, the model/apparatus provides for a solid foundation for further testing and experiments. Certain improvements should be considered in order to advance the model further as discussed below.

The new model is an advancement to the previous set-up. The tests have demonstrated signatures better resembling RTDD data for normal hook load curves, including the important static friction first peak.The new set-up also has an improved position acquisition rate where the position can be measured at the same rate as the hook load and flow. The increased pulling force of the model

is its advantage and disadvantage at the same time. The heavy load meant that the model was placed close to the ground in order to have better control of the tension forces. Raising the model would have meant building an extensive and expensive steel structure to handle the load. As a consequence, problems related to flow through the pipes occurred.

The model has a flow meter for measuring flow through the pipe, which the previous model did not; the flow however carries large uncertainties because the seals at the end of the pipes are not watertight. This was a conscious decision. The seal grips onto the wire and increases friction during tripping. If the seals were tighter, the friction from the seals would become the main contributor of friction rather than the forces inside the pipe. This is already a concern as the friction from the seals add to the pulling force around 3-4 kg. Because the model is placed at ground level the water flow out has to overcome gravity in order to exit the pipe. A solution would be to elevate the entire design. 5-10 cm should be sufficient and not require much structural change to the design. This would allow the water out to use gravity to its advantage, and lower the pressure on the seals. In the current situation, the flow leaks out of the edges of the pipe, especially when restrictions from cuttings and BHA cause the pressure to build behind the restriction.

The model encompasses increased pulling force capacity and safety features to safeguard its operation, as well as flexibility with respect to key parameter variations. Consequently, the set-up might come across as somewhat difficult and time consuming to use by new users. Procedures have therefore been carefully explained in chapter 6 in order to improve user friendliness. However, it is unavoidable that setting up a large scale operation with the forces involved takes time. Once the set-up has been used a few times the user can set-up a completely new experiment in 10-20 min.

In regards to the LabVIEW program it is well-presented and easy to grasp. The next step is to build a more complex mathematical model for the theoretical hook load then the one currently in LabVIEW. The only variable current in the equation is fluid drag and the model is not dynamic with regards to block position. Variables to include in further modeling would be

- Acceleration
- Flow rate in annulus

- Block postion

8.2 Evaluation of Results

Several of the tests showed promising results. The results resembled RTDD data for normal hook load, cuttings accumulation, and for moving past an obstacle. Figure 46 illustrates three curves from the experiment. The two upper figures are expressed via excel for easier recognition in the same manner as Bjerke's (2013) recognition model. Bjerke focuses only on the hook load. The lower figure shows the hook load signature for moving past an obstacle. As this trial was not recorded in excel, a comparable graph focusing on hook load was not created. We can see that the sudden spike followed by a drop resembles the restriction for a fixed restriction from Bjerke's recognition model. Despite the similarities, this bottom figure was a result of the BHA moving past cuttings, which is normally a moveable restriction. In support of Bjerke's theory, if the BHA simply caught on to a few large cuttings and then proceeded to slide over, then the case for practical purposes resembled a fixed restriction. The hook load curve supports this theory.

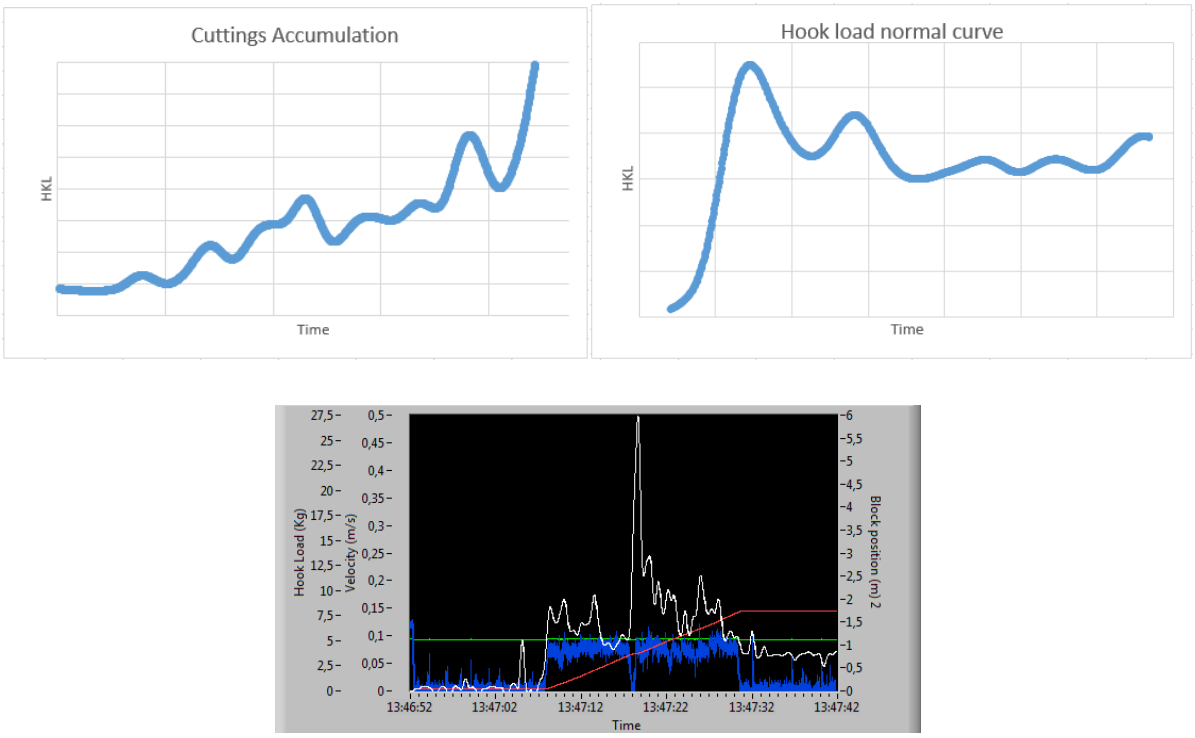

Figure 46: Figures resembling the established fingerprint for cuttings accumulation (upper left) normal hook load curve (upper right) and moving past a restriction (lower figure).

The results largely support what has been established in the literature study. This gives further evidence that the research conducted in recent years at NTNU, in this thesis and others, bears fruit. If the rig and knowledge gained so far are properly developed further, the potential of finding causes and symptom recognition tools of value for the industry is present.

The stuck pipe due to cuttings accumulation was purposely created in this thesis. This was in order to present an absolute signature. From the established RTDD signatures and the observations during the experiment, there can be no doubt that this is a signature for cuttings accumulation. This means the hook load rig is capable of creating signatures for cuttings accumulation.

The next step is to create a case where the signature matches the cuttings accumulation established in this thesis, but overcomes the obstacle. In a tripping situation, this is the most common result of an overpull. This is vital in order to establish early detection models.

However, it is the author's personal belief that the stuck pipe case can prove valuable in creating symptom recognition models. The build-up of hook load is evident over a period and it should be

possible create mathematically a warning before the pipe becomes stuck. Severe cases, as well as cases where the obstacle was overcome, are important in qualifying early detection models.

Each result presented here was tested several times before the graphs could be qualified as valid. However, there are several uncertainties in the results. The largest uncertainties are connected to the frequency problem previously mentioned and presented several times in the thesis.

When the problem arose, contact was made with Ståle Færøy, offshore electrician specialist for Transocean. An important aspect of reducing noise is to supply power to equipment from different power networks. This is usually solved by isolating the power networks from each other. In addition, for frequency-based transducers the frequency may be shifted to another range, altering it from its normal sinus curve. It is usually shifted ± 7,5 degrees.

Færøy's main suggestions to reduce noise were followed and included grounding of equipment, adding net-filter to frequency drive and isolating the load cell from metal contact. Another tip was to keep cables separated as they often induce noise when in close contact, especially when twined together. This proved to be true. In this set-up it is particularly important to keep the cable from the control unit of the winch and the cable to the load cell separated. Figure 47 illustrates the noise on the hook load signal in a state of no movement and no tension on the drillstring. The figure should lie still at 0 kg. At the middle of the graph, the power for the frequency drive is shut off.

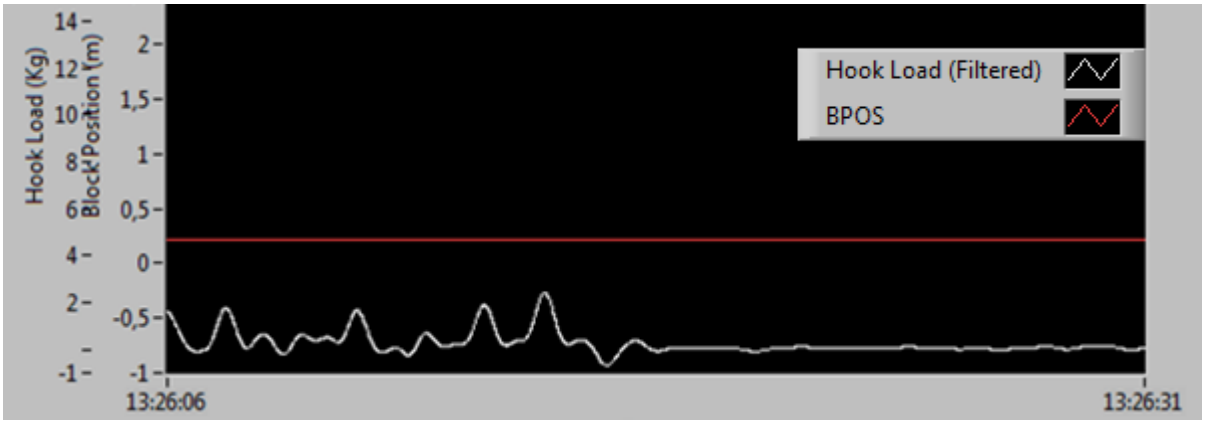

Figure 47: Interference on the hook load signal. At the midpoint in the graph, the frequency drive for the winch is shut off. The curve establishes itself at exactly 0 kg.

The filters which are installed in LabVIEW are another cause of uncertainties. The smoothing filter is currently set at an average over the 20 last measurements. At a rate of 100 Hz this is acceptable as it averages out any anomalies. However, this explains also why at 3 Hz, the curve showed little resemblance to the one at 100 Hz (figure 43 above). At 3 Hz the average over the 20 last measurements simply means that almost the entire curve is averaged out and no real dependable data can be read through the graph. Tests were also conducted with a lower number of data points to obtain smoothing average, but the only real difference was that the noise became more observable. The problem with smoothing the recordings is that a large increase over a short period of time will be heavily dampened.

In discussions with Åge Sivertsen, responsible for electrical equipment at the IPT-hall, he informed that the electrical system currently available in the laboratory is poor. In order to produce less noise the entire electrical system at IPT is in need of an upgrade.

After the noise had been reduced to a few kg, Tor Inge Waag, who has a Ph.D. in measurement technology, was contacted about the issue. Most of his suggestions for reducing noise had already been tried. He concluded that as far as he could tell, the final step to take would be to replace the load cell. The 2000kg load cell was switched out with a 200 kg load cell. The idea was that the voltage output would be larger at less weight and therefore less sensitive to noise. However, the load cell proved to be equally sensitive and could sustain less load. A switch was made back to the 2000 kg load cell for the remaining experiments.

An interesting observation was that when the winch started pulling on the string, the noise was further reduced as long as the winch was in rotation. Neither expert could explain this phenomenon without further investigation.

It is worth a final comment that in the current set –up the noise varied between 1-2 kg, in worst cases 4 kg. When dealing with restriction tests this value becomes a non-factor, when the pulling force rose above 100 kg. In addition, at loads as low as 20 kg the variation becomes minute. It is only when working with the BHA and drillpipe weight alone this became an issue. Even then, the trends were clear and observable, as established chapter 7. However, the goal is always to reduce as many noise inputs as possible. That is why this issue was given effort and time.

8.3 Further work

Several suggestions for improvements have been presented in the evaluation section above. This section will be a quick summary of suggested improvements for the hook load rig:

- Introduce a pressure sensor at the back of the pipe to simulate SPP increase from RTDD when flow in is constant
- Lift the entire set-up 5-10 cm to improve flow conditions
- Evaluate and resolve leaking flow problem
- It is difficult to determine borehole restrictions by simply looking at hook load signatures, other parameters such as torque, pressure and flow are important in developing hook load recognition models

In addition, it is suggested that the model be tested for restrictions that are passable, i.e. a cuttings accumulation test that overcomes the obstacle.

The main goal of building the new hook load rig is for future development of problem recognition tools. The next step is to solve the challenges above and create more cases that match RTDD data. The mathematical predictive model will have two phases:

1. Further development of hook load behavior during normal tripping that can be simulated on the laboratory model, such as Mme's mass-spring model.
2. Creating a detection system for any anomalies outside of expected hook load force

The hook load rig in the laboratory in its current state resembles a borehole with a drillstring in it. The model is therefore not limited to hook load testing. Other uses could include:

- Cuttings transport
- Pressure in well
- Friction factor estimation
- Cling factor
- Drillstring velocity, etc.

9 Conclusion

The following conclusions have been drawn based on the findings during the course of this thesis:

- Through study of hook load signatures from RTDD and literature, signature curves for hook load have been established.
- The hook load rig was tested and qualified and issues such as frequency disturbances were dealt with and largely resolved.
- Other parameters such as torque, pressure and flow need to be included in recognizing causes for restrictions in the borehole.
- The test result provide support to previous theories related to hook load signatures
- Initial testing shows hook load signatures resembling hook load curves from RTDD for
    - Normal hook load curve
    - Cuttings accumulation
    - Moving over an object
- Improvements to the built hook load rig are necessary for development of mathematical hook load models.

10 Nomenclature

BHA	Bottom hole assembly
BPOS	Block position
CoF	Coefficient of Fraction
DLS	Dog-leg severity
DBTM	Measured depth of the drill bit
HKL	Hook load
MDI	Mud density in
MFI	Mud flow in
MFO	Mud flow out
NPT	Non-productive time
POOH	pulling out of hole
RIH	Run in hole
RKB	Rotary kelly bushing
RPMB	Rounds per minute of the drillstring
RTDD	Real-time drilling data
SPP	Stand pipe pressure
TRQ	Torque in the borehole
TVD	True vertical depth
WOB	Weight on Bit

A_{cs}	Cross section area
F_{axial}	Axial force
F_D	Fluid drag
F_{dl}	Deadline tension
F_f	Friction force
F_n	Normal friction
L	Length of element
V	Voltage
d_h	Diameter of annulus
d_s	Diameter of drillpipe
m	Mass
q	Flow
v	Velocity
w	Weight of drillstring
α,θ	Inclination
β	Buoyancy
μ	Friction
ε	Strain
σ	Stress
φ	Local dog-leg
ρ	Density

11 Bibliography

Aadnoy, B., & Davy, C. (2010). *Advanced Drilling and Well Technlogy-Compendium in High Deviation Drilling.* NTNU.

Aarrestad, T., & Blikra, H. (1994). Torque and Drag-Two Factors in Extended-Reach Drilling. *Journal of Petroleum Technology. Vol 46. Number 9. ISBN 27491-PA, Vol 4*(9).

Aarsland, S. (2012). *Torque Evalutation Well 34/10-C-47.* NTNU.

Aker Solutions. (2013). *Hoisting systems Manual*. Retrieved from akersolutions: http://www.akersolutions.com/Documents/Drilling%20Technologies/MH%20products/2012/2%20Hoisting%20systems.pdf

Bjerke, H. (2013). *Revealing Causes of Restrictions by Signatures in Real-Time Hook Load Signals.* NTNU-Department of Petroleum and Applied Geophysics.

Booth, J. (2011). *Real Time Drilling Operations Centers: A History of funtionality and organizational Purpose-The Second Generation.* SPE.

Cordoso Jr, J. V., Maidla, E., & Idagawa, L. (1995). Problem Detection During Tripping Operations in Horizontal and Directional Wells . *SPE*, 77-83.

Drilling Contractor. (2014). *http://www.drillingcontractor.org*. Retrieved from http://www.drillingcontractor.org/remote-operations-centers-earning-keep-through-drilling-optimization-247-support-%E2%80%98remanning%E2%80%99-6816

Fazaelizadeh, M., Aadnoy, B., & Hareland, G. (2010). *Application of New 3-D analytical Model for Directional Wellbore Friction.* CCSE.

Freithofing, H., TDE, Sporeker, & 3et.al. (2003). Analysis of Hook Load Data to Optimize Ream and Wash Operations. (pp. 1-11). Abu Dabi, UAE: SPE/IADC 85308.

Glomstad, T. (2012). *Analysis of Hook Load Signal to Reaveal the Causes if Restrictions.* NTNU, Department of Petroleum Engineering and Applied Geophysics.

Etomica. (2014). *Etomica*. Retrieved from http://www.etomica.org/app/modules/sites/MaterialFracture/Images/SSPicture1.jpg

Johancsik, C., Friesen, D., & Dawson, R. (1984, June). Torque and Drag Deviation in Wells-Prediction and Measurment. *Journal of Petroleum Technology,* 987-992.

Kristensen, E. (2013). *Model of Hook Load During Tripping Operation.* Trondheim: NTNU-Department of Petroleum an Applied Geophysics.

Luke, G., & Juvkam-Wold, H. (1993, December). Determination of the True Hook Load Under Dynamic Conditions. *SPE,* 259-264.

Maidla, E. E., & A.K., W. (1987). Field Comparison of 2D and 3D Methods for the Borehole Friction Evaluation in Directional Wells. *SPE,*16663

Maidla, E., & Wojtanowicz, A. (1987, March). Field Method of Assesing Borehole Friction for Directional Well Casing. *SPE,* 85-96, 15696

Offshore.no. (2014, Januar). *Offshore.no*. Retrieved from http://offshore.no/Prosjekter/riggdata.aspx

PetroWiki. (2014). *Mechanical Stuck Pipe*. Retrieved from PetroWiki: http://petrowiki.org/index.php?title=Mechanical_pipe_sticking&printable=yes

Polak, M., & Lasheen, A. (2002). Mechanical Modelling in Pipes for HorizonntalDirectional Drilling. *Tunnelling and Underground Space Technology, 16,* pp. 47-55.

Sangesland, S. (2011). *Torque and Drag Models Lecture Notes.* NTNU.

Schlumberger. (2014). *http://www.glossary.oilfield.slb.com*. Retrieved from http://www.glossary.oilfield.slb.com/en/Terms.aspx?LookIn=term%20name&filter=hook%20load

Skalle, P., & Johanssen, S. T. (Unpublished). *Abnormal Hook Load Response During Tripping Operations.*

Statoil. (2007). *Final Well Raport Well 34/10-C-47.*

Townsend, B. (2002). *The Physics of Car Collions*. Retrieved from http://ffden-2.phys.uaf.edu/211_fall2002.web.dir/ben_townsend/PhysicsofCarCollisions.htm

Wikipedia. (2014). *Wikipedia*. Retrieved from Wikipedia: http://en.wikipedia.org/wiki/Drill_floor